Nucleation, adatom capture, and island size distributions: Unified scaling analysis for submonolayer deposition

J. W. Evans[1] and M. C. Bartelt[2]
[1]*Department of Mathematics and Ames Laboratory, Iowa State University, Ames, Iowa 50011*
[2]*Department of Chemistry and Materials Science, Lawrence Livermore National Laboratories, Livermore, California 94550*
(Received 18 December 2000; published 25 May 2001)

We consider the irreversible nucleation and growth of two-dimensional islands during submonolayer deposition in the regime of large island sizes. A quasihydrodynamic analysis of rate equations for island densities yields an ordinary differential equation (ODE) for the scaling function describing the island size distribution. This ODE involves the scaling function for the dependence on island size of ''capture numbers'' describing the aggregation of diffusing adatoms. The latter is determined via a quasihydrodynamic analysis of rate equations for the areas of ''capture zones'' surrounding islands. Alternatively, a more complicated analysis yields a partial differential equation (PDE) for the scaling function describing the joint probability distribution for island sizes and capture zone areas. Then, applying a moment analysis to this PDE, we obtain refined versions of the above ODE's, together with a third equation for the variance of the cell area distribution (for islands of a given size). The key nontrivial input to the above equations is a detailed characterization of nucleation. We analyze these equations for a general formulation of nucleation, as well as for an idealized picture considered previously, wherein nucleated islands have capture zones lying completely within those of existing islands.

DOI: 10.1103/PhysRevB.63.235408 PACS number(s): 68.55.Jk, 81.15.Hi, 05.40.−a

I. INTRODUCTION

For decades, there has been interest in characterizing island formation during the initial stages of film growth. [1,2] Of particular interest is the nature of the island size distribution. There are heuristic predictions for this distribution going back to the earliest theoretical analyses,[1,2] self-consistent mean-field rate-equation treatments,[3,4] subsequent postulated analytical forms,[5] and also simple geometric interpretations based on adatom capture.[6] However, each of these fails to recover key qualitative features observed in precise simulation results for the size distribution.[4] Key to a resolution of these shortcomings is recognizing that this size distribution is controlled by the non-mean-field (non-MF) dependence on island size s (measured in atoms) of the ''capture numbers'' σ_s.[6,7] These capture numbers describe the propensity of islands to capture diffusing adatoms. Most significantly, we were able to obtain an explicit and *exact formula*, which relates the shape of the island size distribution to the behavior of the capture numbers,[7] thus providing a much sought-after theory for explaining this shape.

The remaining challenge is to understand the non-MF dependence of σ_s. Some insight comes from a geometric picture of adatom capture in terms of ''capture zones'' which surround each island.[6–9] The idea is that atoms deposited within such a capture zone will typically aggregate with the associated island. The main observation is that larger islands have larger capture zones.[6–9] This implies the existence of a correlation between island size and separation, which is ignored in MF treatments. As an aside, the problem of constructing capture zones which precisely reflect adatom capture leads to an analysis of an appropriate continuum diffusion equation for deposited atoms. This procedure is central to developing continuum treatments of island growth, i.e., in connecting atomistic and mesoscopic length scales.[8–10]

To date, there have been two significant attempts to explain the form of σ_s versus s. These include our previous rate-equation formulation for mean capture zone areas versus island size,[11] and a more complicated analysis of the joint probability distribution for island size and capture zone areas by Mulheran and Robbie.[12] However, a quantitatively precise theory has yet to be developed. It is clear that the early nucleation stage is crucial, noting, for example, that islands nucleated earlier tend to have larger capture zones.[7] Furthermore, recent studies reveal a strong sensitivity of the island size distribution to the prescription of nucleation.[13] Thus a sophisticated characterization of the nucleation process is key to a comprehensive understanding of adatom capture and island size distributions.

To this end, we consider the simplest regime of irreversible island formation during submonolayer deposition. Our discussion will focus on the common case of compact two-dimensional islands, further restricting attention to the precoalescence regime. We shall also consider and show results for the special case of ''point islands.'' In the latter idealized model, islands occupy a single site on the lattice, but carry a label indicating their size.[4] This idealized model is useful for elucidating scaling behavior at low coverages. In both cases, the key atomistic processes involved are as follows. Atoms are deposited at random at a rate F per site, and subsequently undergo terrace diffusion with a hop rate h (per direction). This leads to the irreversible nucleation of islands when two diffusing adatoms meet. Also, existing islands grow due to irreversible aggregation of diffusing adatoms, and due to the incorporation of atoms deposited directly on top of islands. In this analysis, we regard the latter process as instantaneous. The fundamental quantities of interest are the densities (per adsorption site) of islands of s atoms, which are denoted by N_s (so N_1 gives the density of diffusing atoms), the average island density denoted by $N_{\rm av}=\Sigma_{s>1}N_s$, the coverage by $\theta=\Sigma_{s\geq 1}sN_s$, and the average island size (measured in atoms) by $s_{\rm av}=(\theta-N_1)/N_{\rm av}\approx\theta/N_{\rm av}$. Below, we shall consider ex-

clusively the *scaling regime* of large s_{av}.

In Sec. II, we first present the standard rate equations for evolution of the island densities. We then apply to these a quasihydrodynamic analysis, treating the scaled island size s/s_{av} as a continuous variable (denoted by x). This yields an ordinary differential equation (ODE) for the scaling function describing the island size distribution in terms of that for capture numbers (or capture zone areas). We extend our previous derivation for point islands[7] to the case of compact islands, and also present several basic relations for the scaling functions. Next, in Sec. III, we develop approximate rate equations for capture zone areas, and again perform a quasihydrodynamic analysis to obtain an ODE for the associated scaling function. This extends our previous formulation in Ref. 11. These equations are analyzed for an exact prescription of nucleation, and reproduce the key features of the island size dependence of adatom capture. We also consider a simplified description corresponding to ''nucleation inside a cell,'' where just nucleated islands have capture zones lying completely within those of existing islands. Next, in Sec. IV, following ideas of Mulheran and Robbie,[12] we develop equations describing the joint probability distribution for island sizes and capture zone areas. A quasihydrodynamic analysis yields a partial differential equation (PDE) for the associated scaling function. Applying a moment analysis to this PDE, we recover the above ODE for the island size distribution, and obtain a refined version of the ODE for capture zone areas (where the refinement accounts for the distribution of capture zone areas for islands of a given size). We further obtain a third ODE for the variance of this area distribution. However, the formulation is still not exact, and requires specific input on the nucleation process. A summary and brief discussion of proposed developments in the characterization of nucleation are presented in the concluding Sec. V.

II. ISLAND SIZE DISTRIBUTION: RATE EQUATIONS AND SCALING

A. Basic formulation

In the following, the rate at which diffusing atoms aggregate with islands of size s is denoted by $R_{agg}(s) \equiv h\sigma_s N_s N_1$, defining a dimensionless ''capture number'' σ_s for islands of size s atoms. The total aggregation rate for diffusing atoms satisfies $R_{agg}(\text{total}) = \Sigma_{s>1} R_{agg}(s) = h\sigma_{av} N_{av} N_1$, where $\sigma_{av} = \Sigma_{s>1}\sigma_s N_s / N_{av}$ is the average capture number. The rate of direct deposition on top of islands of size s is denoted by $R_{dep}(s) \equiv F\kappa_s N_s$. This relation defines the direct capture number $\kappa_s \approx s$ for compact islands, neglecting possible perimeter corrections of order $s^{1/2}$ ($\kappa_s \sim 1$ for point islands). Then, if $R_{tot}(s) = R_{agg}(s) + R_{dep}(s)$, the rate equations for the evolution of the island densities N_s have the form [1,2,5–7]

$$\begin{aligned} d/dt N_s &= R_{agg}(s-1) - R_{agg}(s) + R_{dep}(s-1) - R_{dep}(s) \\ &= R_{tot}(s-1) - R_{tot}(s), \quad \text{for } s>1. \end{aligned} \tag{1}$$

The equation for N_1 involves a gain term due to deposition (excluding on-top deposition events), loss terms due to aggregation with islands of all sizes $s>1$, and others due to nucleation. Contracting this equation for N_1 (neglecting loss due to nucleation), and the equation for N_{av}, yields

$$d/dt\ N_1 \approx F(1-\theta) - R_{agg}(\text{total})$$

and

$$d/dt\ N_{av} \approx h\sigma_1 (N_1)^2. \tag{2}$$

Thus in the steady-state regime where adatom gain and loss roughly balance, one has

$$F(1-\theta) \approx h\sigma_{av} N_{av} N_1. \tag{3}$$

This steady-state relation can be used to integrate the N_{av} equation yielding $N_{av} \sim G(\theta)(h/F)^{-1/3}$. Here, the nontrivial θ dependence of $G(\theta)$ reflects that of σ_{av} and σ_1.[3] If this dependence is weak, then one obtains $G \sim \theta^{\omega}$ with $\omega = \frac{1}{3}$. This implies that $s_{av} \sim \theta^{\omega}(h/F)^{1/3}$, where $\varpi = 1-\omega$, and thus $\varpi = \frac{2}{3}$. Scaling with $\varpi = \frac{2}{3}$ applies for point islands,[4] whereas one tends to find effective values of ϖ closer to (but below) unity for compact islands.[8,9] This latter feature reflects a greater inhibition of nucleation due to the finite extent of the compact (versus point) islands. However, we believe that for compact islands with sufficiently small θ, point-island behavior where $\varpi = \frac{2}{3}$ would eventually be recovered in the scaling regime (for very large h/F or s_{av}).

B. Quasihydrodynamic scaling analysis

In this scaling regime of large s_{av}, we introduce the natural variable $x = s/s_{av}$, and perform a quasihydrodynamic analysis treating x as a continuous variable. We write the island densities in the general scaling form[4] $N_s \approx N_{av}(s_{av})^{-1} f(x,\theta) \approx \theta(s_{av})^{-2} f(x,\theta)$, where the constraints $\int_0^\infty dx\, f(x,\theta) = \int_0^\infty dx\, x f(x,\theta) = 1$ ensure that the above normalization conditions are satisfied. One could also write $\sigma_s/\sigma_{av} \approx C_{agg}(x,\theta)$, where $\int_0^\infty dx\, C_{agg}(x,\theta) f(x,\theta) = 1$. In choosing these forms, we have allowed (at this stage) for the possibility of an explicit θ dependence in the scaling functions. For *compact islands*, where $\kappa_s/\kappa_{av} \approx s/s_{av} = x$, one can show that (cf. Refs. 7 and 14)

$$\begin{aligned} d/dt N_s &\approx F(s_{av})^{-2}[(1-2\varpi)f - \varpi x \partial f/\partial x + \theta \partial f/\partial\theta], \\ R_{agg}(s) - R_{agg}(s-1) &\approx \partial/\partial s R_{agg} \\ &\approx F(s_{av})^{-2}(1-\theta)\partial/\partial x (C_{agg} f), \\ R_{dep}(s) - R_{dep}(s-1) &\approx \partial/\partial s R_{dep} \approx F(s_{av})^{-2}\theta \partial/\partial x (xf), \\ R_{tot}(s) - R_{tot}(s) &\approx F(s_{av})^{-2}\partial/\partial x (C_{tot} f). \end{aligned} \tag{4}$$

Here Eq. (3) is used to analyze the R_{agg} term. We have defined $\varpi = d(\ln s_{av})/d(\ln\theta)$, and ignored any θ-dependence of ϖ. We also naturally combine aggregation and on-top deposition terms into a single natural scaling function, $C_{tot}(x,\theta) \equiv \theta x + (1-\theta) C_{agg}(x,\theta)$. The above normalization conditions on f and C_{agg} imply the further normalization condition that $\int_0^\infty dx\, C_{tot}(x,\theta) f(x,\theta) = 1$. One thus obtains the *fundamental equation*

$$(1-2\varpi)f-\varpi x\partial f/\partial x+\theta\partial f/\partial\theta=-\partial/\partial x(C_{\rm tot}\,f). \quad (5)$$

We emphasize that Eq. (5) is an *exact* relation. For *point islands*, one has $\kappa_s/s_{\rm av}\approx 0$, and naturally defines $C_{\rm tot}(x)\equiv C_{\rm agg}(x)$, so Eq. (5) still applies (cf. Ref. 7).

If $C_{\rm tot}$ has no explicit θ dependence, then it follows that a solution of the partial differential equation (PDE) (5) subject to the normalization constraints mentioned above is selected with f independent of θ. See Ref. 10 for a more detailed discussion. In this way, we recover the well-known θ-independent scaling form for f versus x observed previously in simulations.[4] Furthermore, in this case, $f(x)$ can be determined by integrating the ODE obtained by dropping the $\partial/\partial\theta$ term in Eq. (5). One thus obtains

$$f(x)=f(0)\exp\left\{\int_0^x dy[(2\varpi-1)-d/dy\,C_{\rm tot}(y)]/[C_{\rm tot}(y)-\varpi y]\right\}, \quad (6)$$

extending the result of Ref. 7. Equation (6) can be rewritten as (cf. Ref. 10)

$$f(x)=f(0)C_{\rm tot}(0)[C_{\rm tot}(x)-\varpi x]^{-1}\times\exp\left\{-(1-\varpi)\int_0^x dy[C_{\rm tot}(y)-\varpi y]^{-1}\right\}. \quad (7)$$

Here $f(0)$ is chosen to ensure that $\int_0^\infty dx\,f(x)=1$. Typically, our focus will be on the regime of low $\theta\ll 1$, where $C_{\rm tot}\approx C_{\rm agg}$ (or on the case of point islands, where $C_{\rm tot}\equiv C_{\rm agg}$), so θ-independent scaling derives from that of the scaling function, $C_{\rm agg}(x)$, for the capture numbers.

C. Properties of the scaling function $f(x)$

In this subsection, we consider only the case of *θ-independent scaling*. We shall see below that both $C_{\rm agg}(x)$ and $C_{\rm tot}(x)$ exceed ϖx, for small x. Then it is clear from Eq. (6) or Eq. (7) that the form of $f(x)$ depends sensitively on whether or not $C_{\rm tot}(x)$ exceeds ϖx, for *all* x. Thus we now examine the different possible scenarios in more detail.

First, suppose that $C_{\rm tot}(x)-\varpi x>0$, for all x, and that $C_{\rm tot}(x)\sim\upsilon\kappa$, for large x, with $\upsilon>\varpi$. Then, from Eq. (6), it immediately follows that

$$f(x)C_{\rm tot}(x)\sim f(0)C_{\rm tot}(0)x^{-(1-\varpi)/(\upsilon-\varpi)} \quad \text{as } x\to\infty,$$
$$\text{so } (1-\varpi)/(\upsilon-\varpi)>1 \text{ or } \upsilon<1. \quad (8)$$

The latter condition is *required* to ensure convergence of the integral $\int_0^\infty dx\,f(x)C_{\rm tot}(x)=1$. The inequality $\upsilon<1$ constitutes an important constraint on the behavior of the capture numbers. Note that the unphysical form $C_{\rm tot}(x)=x$ can be associated with the complete absence of nucleation,[15] indicating the importance of continuous nucleation in determining the form of $f(x)$. If $C_{\rm tot}(x)>\varpi x$, and $C_{\rm tot}(x)-\varpi x\to$const (>0), or $C_{\rm tot}(x)-\varpi x\to 0+$, as $x\to\infty$, then one can show that $f(x)C_{\rm tot}(x)\to 0$, as $x\to\infty$, sufficiently fast to ensure normalization.

Second, suppose that $C_{\rm tot}(x)-\varpi x\to 0+$, as $x\to x^*$ $(<\infty)$ from below. Then, one has that $f(x)\equiv 0$ for $x>x^*$, and, from Eq. (7), that

$$f(x)\sim(x^*-x)^\gamma$$
$$\text{where } \gamma=[d/dx\,C_{\rm tot}(x^*)-(2\varpi-1)]/[2\varpi-d/dx\,C_{\rm tot}(x^*)] \quad \text{for } x<x^*. \quad (9)$$

There are two distinct cases to consider. If $d/dx\,C_{\rm tot}(x^*)>2\varpi-1$ (so $\gamma>0$), then $f(x)\to 0$, as $x\to x^*$ from below. If $d/dx\,C_{\rm tot}(x^*)<2\varpi-1$ (so $\gamma<0$), then $f(x)$ diverges as $x\to x^*$ from below. The latter corresponds to unphysical mean-field-type behavior.[7–11]

Finally, we comment on some basic normalization issues. Simply applying the operation $\int_0^\infty x^n dx\cdot$ to Eq. (5) (after dropping the $\partial/\partial\theta$ term) yields the key relations[16]

$$(1-\varpi)\int_0^\infty dx\,f(x)=f(0)C_{\rm tot}(0)\ \ (=1-\varpi) \quad \text{for } n=0, \quad (10a)$$

$$\int_0^\infty dx\,xf(x)=\int_0^\infty dx\,C_{\rm tot}(x)f(x)\ \ (=1) \quad \text{for } n=1, \quad (10b)$$

$$(1+\varpi)\int_0^\infty dx\,x^2f(x)=2\int_0^\infty dx\,xC_{\rm tot}(x)f(x) \quad \text{for } n=2. \quad (10c)$$

The result for $n=0$, that $f(0)C_{\rm tot}(0)=1-\varpi$, provides a key constraint on the behavior of $f(x)$ and $C_{\rm tot}(x)$ for small island sizes. Substitution into Eq. (7) simplifies this expression for $f(x)$, and further demonstrates the requirement that $\varpi<1$. The result for $n=1$ ensures that normalization of the scaling functions is consistent with the conditions on $C_{\rm tot}(x)$ stated above. The result for $n=2$ provides insight into the variance σ_f^2 of the scaling function for the island size distribution:

$$\sigma_f^2=\int_0^\infty dx(x-1)^2f(x)$$
$$=2(1+\varpi)^{-1}\int_0^\infty dx\,xC_{\rm tot}(x)f(x)-1$$
$$=2(1+\varpi)^{-1}\int_0^\infty dx[x-\tfrac{1}{2}(1+\varpi)]C_{\rm tot}(x)f(x)$$
$$>(1-\varpi)/(1+\varpi). \quad (11)$$

For the last inequality, we have used that $\int_0^\infty dx\,xC_{\rm tot}(x)f(x)>1$. This quantity is the mean of the normalized distribution $C_{\rm tot}(x)f(x)$, which should exceed the mean (of unity) of the normalized distribution f, due to the feature that $C_{\rm tot}(x)$ is a monotonically increasing function (see below).

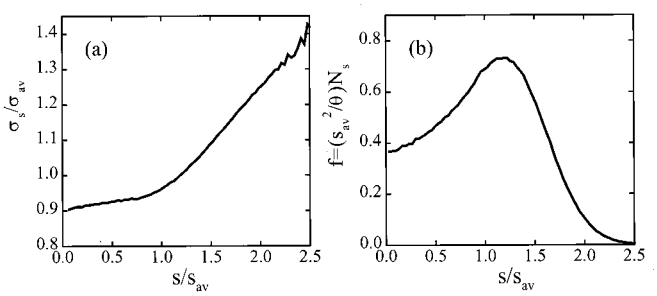

FIG. 1. (a) Capture number behavior, and (b) island size distribution for the point-island model at 0.1 ML with $h/F=10^7$.

D. Simulation results for scaling functions

It is appropriate here to review previous simulation results for both point and compact islands with large h/F, which elucidate the forms of $f(x)$, and $C_{agg}(x)$ or $C_{tot}(x)$. These will provide a benchmark for our subsequent analyses. In Fig. 1(a), we show results for $C_{agg}(x)\approx\sigma_s/\sigma_{av}$ versus s/s_{av} for *point islands* at 0.1 ML with $h/F=10^7$ (a value used throughout this work). These results indicate that $C_{tot}(x)\equiv C_{agg}(x)$ exhibits a plateau for $x<1$ (roughly), followed by a quasilinear increase for $x>1$ with $C_{agg}(x)\sim\upsilon x$, and $\upsilon\approx\frac{2}{3}$ (with considerable uncertainty in υ). It is not clear whether the true asymptotic form of $C_{agg}(x)$ crosses $\varpi x=2x/3$. However, if it does, its derivative certainly exceeds $2\varpi-1=\frac{1}{3}$ at the crossing point, so the island size distributions shown in Fig. 1(b) reveal that $f(x)$ exhibits no singularity. Results show that $f(0)\approx0.35$ is nonzero, contrasting proposals in Refs. 5 and 6. Also, since $C_{tot}(0)\approx0.91$, the behavior is consistent with Eq. (10a) given that $\varpi=\frac{2}{3}$.

In Fig. 2(a), we show results for $C_{tot}(x)\approx\theta\kappa_s/\kappa_{av}+(1-\theta)\sigma_s/\sigma_{av}$ vs s/s_{av} for *square islands* at 0.1 ML with $h/F=10^7$. These results indicate much less of a plateau in $C_{tot}(x)$ than for point islands, and a steeper increase for $x>1$ with υ closer to unity. The behavior of $C_{agg}(x)$ is similar.[14] The island size distributions for square islands, shown in Fig. 2(b), are similar to those for point islands. These differences in the form of $C_{tot}(x)$ for compact and point islands may to some extent reflect nonasymptotic behavior for compact islands deriving from the non-negligible θ, and finite h/F used in the simulations. For non-negligible θ, nucleation is inhibited for compact islands compared to point islands (with the same nominal θ), forcing an effective ϖ close to unity, and perhaps forcing behavior closer to $C_{tot}(x)\approx x$ (corresponding to the absence of nucleation). This issue will be explored in detail in a separate paper focusing on simulation results. We also note that behavior for compact islands is expected to be roughly independent of their shape. See Ref. 8 for corresponding results for hexagonal islands. Finally, it should be emphasized that the observed small-x behavior, where $f(0)\approx0.35$ and $C_{tot}(0)\approx0.4$, is again consistent with Eq. (10a) using the observed effective $\varpi\approx0.9$.

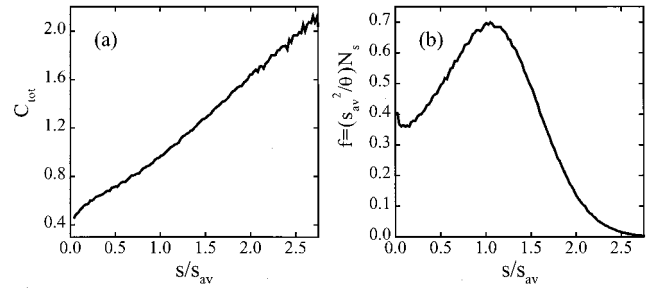

FIG. 2. (a) Capture number behavior, and (b) island size distribution for the square-island model at 0.1 ML with $h/F=10^7$.

III. CAPTURE ZONE AREAS: RATE EQUATIONS AND SCALING

A. Basic formulation

Intuition suggests that most deposited atoms should aggregate with nearby islands. Thus, as indicated in Sec. I, it is natural to construct a tessellation of the surface into cells or ''capture zones'' based on the island distribution, so that each cell contains a single island. Specific choices of tessellations will be discussed in Sec. III C. In all cases, the mean area for cells corresponding to islands of size s (including the area of the enclosed island) is denoted by A_s (in units of adsorption site area), so $A_{av}=\Sigma_{s>1}A_sN_s/N_{av}=1/N_{av}$. For compact islands, it is appropriate also to introduce the ''free areas,'' $A_s^f=A_s-s$, of the cells, which exclude the island area, so then $A_{av}^f=(1-\theta+N_1)A_{av}\approx(1-\theta)A_{av}$. For point islands, one has $A_{av}^f\approx A_{av}$.

One might anticipate that the dependence of A_s on island size s would provide basic insight into the form of σ_s versus s, and thus the form of $C_{agg}(x)$. Bales[17] suggested developing rate equations for A_s as a way to assess their dependence on s. As a first attempt to resolve this central issue in nucleation theory, we previously developed such rate equations for the A_s for point islands in Ref. 11, and furthermore developed the quasihydrodynamic scaling form of these equations. Here we present a more general derivation, discuss the approximations inherent in such equations, and also analyze the behavior of the solutions of these equations.

For compact islands, we consider the fractional area A_sN_s of cells associated with islands of size $s>1$. Changes in this quantity occur primarily for two reasons: (i) islands increase their size in increments of $\delta s=1$ due to aggregation or direct on-top deposition, thus shifting cells to islands of larger size; and (ii) when new islands (of size 2) are nucleated, some of the area is removed from the cells of existing islands. See Fig. 3 for a schematic of these processes. The first contributions are easy to treat (approximately), but the latter requires a more detailed characterization of the nucleation process. For this purpose, we let A_{avnuc} denote the *average* cell area associated with just-nucleated islands. We also let P_s denote the typical fraction of the area A_{avnuc} that is removed from the cells of pre-existing islands of size s (per nucleation event). Thus P_s satisfies the normalization condition $\Sigma_{s>1}P_s=1$. Then one has that[11]

$$d/dt(A_sN_s)\approx A_{s-1}R_{agg}(s-1)-A_sR_{agg}(s)+A_{s-1}R_{dep}(s-1)-A_sR_{dep}(s)-A_{avnuc}P_s(dN_{av}/dt)$$

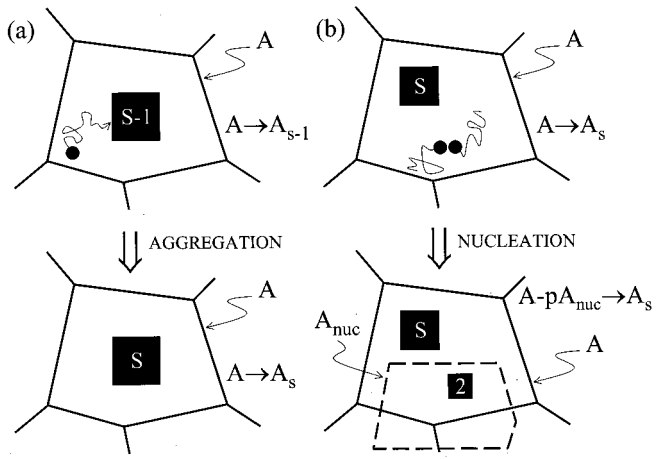

FIG. 3. Schematics for (a) transfer of cells of area A from islands of size $s-1$ to s by aggregation; and (b) reduction of cell area for islands of size s from A to $A-pA_{\rm nuc}$ by nucleation, where p indicates the fraction of the area, $A_{\rm nuc}$, of the nucleated cell by which A is reduced. The notation $\ldots\rightarrow A_s$ associates the area on the left of the arrow with cells of islands of size s.

$$\approx A_{s-1}R_{\rm tot}(s-1)-A_sR_{\rm tot}(s)-A_{\rm avnuc}P_s(dN_{\rm av}/dt) \quad \text{for } s>2. \quad (12)$$

The equation for $d/dt(A_sN_s)$ for $s=2$ has a different form: there is a gain term due to nucleation, and loss terms due to aggregation and direct deposition, (see Appendix A). Finally, we note that the P_s should scale with the density of islands of size s, so we naturally write $P_s=(N_s/N_{\rm av})Q_s$. This factorization will be utilized below.

There are two subtle approximations inherent in formulating Eq. (12). *First*, we ignore the feature that the area of a specific cell typically changes due to a growth of the compact island within the cell, and a growth of the neighboring islands, as this can lead to slight shifts in the location of the cell boundaries.[18] However, we anticipate that the net effect is small. *Second*, we ignore the correlation between the capture zone area and aggregation rate (and between the capture zone area and the direct on-top deposition rate) in replacing ''means of products'' by ''products of means'' in the aggregation and deposition terms in Eq. (12). This approximation will be discussed further in Sec. IV.

Another subtle issue is the identification of $A_{\rm avnuc}$. If the rate of growth of ''dimer'' islands of size $s=2$ greatly exceeds their nucleation rate, then essentially all dimers would be ''just-nucleated islands,'' and $A_{\rm avnuc}$ would correspond to A_2. However, from Eqs. (1) and (2), the rates of dimer nucleation and growth are comparable, so we do not expect this correspondence to be precise. See below for further discussion.

B. Quasihydrodynamic scaling analysis

To perform a quasihydrodynamic analysis of Eq. (12) for compact islands in the regime of large $s_{\rm av}$ we again treat $x=s/s_{\rm av}$ as a continuous variable. We will assume a scaling form $a(x,\theta)\approx A_s/A_{\rm av}$ for cell areas, where $\int_0^\infty dx\, a(x,\theta)f(x,\theta)=1$, and also write $A_{\rm avnuc}/A_{\rm av}=a_{\rm avnuc}$. In Sec. III C, it will also be useful to introduce the scaling form $a^f(x)\approx A_s^f/A_{\rm av}^f$ for free cell areas. Then, since $A_s\approx A_s^f+s$, it follows that $a(x)=\theta x+(1-\theta)a^f(x)$. In addition, below we set

$$P_s\approx(s_{\rm av})^{-1}p(x,\theta) \quad \text{and} \quad Q_s\sim q(x,\theta),$$

$$\text{so } p(x,\theta) \text{ factors as } p(x,\theta)=f(x,\theta)q(x,\theta), \quad (13)$$

where $\int_0^\infty dx\, p(x,\theta)=\int_0^\infty dx\, f(x,\theta)q(x,\theta)=1$.

Using these assumed scaling forms, one can show that

$$d/dt(A_sN_s)\approx -1/(ts_{\rm av})[\varpi\partial/\partial x(xaf)-\theta\partial/\partial\theta(af)],$$

$$A_{s-1}R_{\rm tot}(s-1)-A_sR_{\rm tot}(s)\approx\partial/\partial s[A_sR_{\rm tot}(s)] \approx 1/(ts_{\rm av})\partial/\partial x(aC_{\rm tot}\,f), \quad (14)$$

$$\text{and } A_{\rm avnuc}P_s\ dN_{\rm av}/dt\approx 1/(ts_{\rm av})(1-\varpi)a_{\rm avnuc}qf.$$

Thus it follows that

$$\varpi\partial/\partial x(xaf)-\theta\partial/\partial\theta(af)=\partial/\partial x(aC_{\rm tot}\,f) +(1-\varpi)a_{\rm avnuc}qf. \quad (15)$$

The terms on the left-hand side (LHS) of (15) come from $d/dt(A_sN_s)$, the first term on the right-hand side (RHS) combines aggregation and deposition contributions, and the second term on the RHS comes from nucleation contributions. Again, we focus on solutions of this first-order PDE where $C_{\rm tot}$, and a, q, and f are *independent* of θ (cf. Ref. 10). In this situation, Eq. (15) is simplified by using Eq. (5) (without the $\partial/\partial\theta$ term) to rewrite $\partial f/\partial x$ in terms of f, $C_{\rm tot}$, and $\partial/\partial x(C_{\rm tot})$. After some rearrangement, and cancellation of $\partial/\partial x(C_{\rm tot})$ terms, one obtains the simple ODE

$$[C_{\rm tot}(x)-\varpi x]d/dx\ a(x)=(1-\varpi)[a(x)-a_{\rm avnuc}q(x)]. \quad (16)$$

At this level of treatment, Eq. (16) is the *fundamental equation* for the scaling function describing capture zone or cell areas. It is *not exact*, and its inherent approximations will be described in Sec. IV. This equation also applies for point islands, where $C_{\rm tot}(x)\equiv C_{\rm agg}(x)$.[11,19]

One consequence of Eq. (16), which should be noted here, follows most easily from applying the operation $\int_0^\infty dx\bullet$ to Eq. (15). After dropping the $\partial/\partial\theta$ term, one obtains the relation $a(0)C_{\rm tot}(0)f(0)=(1-\varpi)a_{\rm avnuc}$, where we have used the normalization conditions on $q(x)$. Then, using Eq. (10a), this implies that $a_{\rm avnuc}=a(0)$, which follows if $A_{\rm avnuc}\approx A_2$. As noted above, this corresponds to the scenario where most $s=2$ dimer islands are ''just nucleated,'' a condition which is not precisely satisfied. This problem is addressed in the refined equation for $a(x)$ obtained in Sec. IV.

C. Specific choices of capture zone tessellations

The above formulation applies for any tessellation of the island distribution. The cells in such tessellations might be

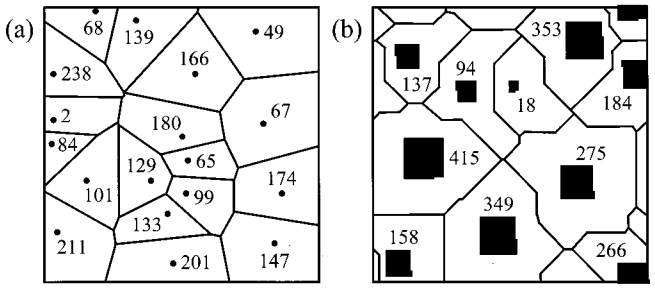

FIG. 4. Examples of (a) a VC tessellation for point islands, and (b) an EC tessellation for square islands. In both cases, $h/F=10^9$, $\theta=0.1$ ML, the picture size is 150×150 sites, and we have indicated the sizes of all islands (in atoms).

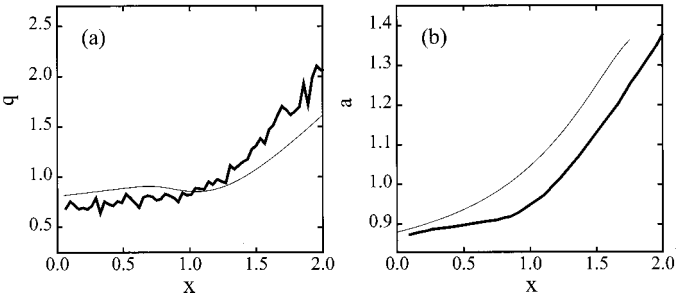

FIG. 5. Simulation results (thick lines) using VC's for the point-island model at 0.1 ML with $h/F=10^7$ for (a) $q(x)$ and (b) the associated $a(x)$. Also shown are predictions obtained from Eq. (16) (thin lines), as described in the text.

generated by *geometric Voronoi-type constructions*. Applying the conventional Voronoi construction, points within the Voronoi cells (VC's) are closer to the centers of the enclosed islands than to the center of other islands. For compact islands at higher coverages, one inadequacy of VC's is that islands may overlap cell boundaries. To avoid this problem and better reflect adatom capture, it is natural for the construction to be based instead on the distance from island edges, producing ''edge cells'' (EC's).[6–9] From analysis of EC's for square islands with ''moderate'' $\theta\approx0.1-0.2$ ML, one finds that[9,16,20]

$$C_{\rm tot}(x)\approx\gamma_s a(x)+(1-\gamma_s),\quad\text{with}\quad\gamma_s\approx1.0$$

$$[\text{i.e.,}\quad C_{\rm tot}(x)\approx a(x)]. \tag{17}$$

For point islands, VC's and EC's are equivalent, and $a^f(x)=a(x)$. Simulation data for point islands reveal that (to quite high precision)[7]

$$C_{\rm tot}(x)=C_{\rm agg}(x)\approx\gamma_p a(x)+(1-\gamma_p),\quad\text{with}\quad\gamma_p\approx0.7. \tag{18}$$

Substitution of Eq. (17) or Eq. (18) for $C_{\rm tot}(x)$ into Eq. (16) yields a ''closed'' equation for $a(x)$, assuming that $q(x)$ is determined independently. Figure 4 shows an example of a VC tessellation for point islands, and an EC tessellation for square islands.

Alternatively, in a more sophisticated choice of tessellation (for either point or compact islands), the cells or capture zones are constructed based on analysis of diffusion equations for deposited atoms, thus precisely reflecting adatom capture. These cells are described as *diffusion cells* (DC's).[8,9,14] By construction, the free area of the diffusion cells is exactly proportional to the capture rate,[8,9] i.e.,

$$\sigma_s/\sigma_{\rm av}=A_s^f/A_{\rm av}^f,\quad\text{so}\quad C_{\rm agg}(x)=a^f(x),$$

$$\text{and thus}\quad C_{\rm tot}(x)=a(x). \tag{19}$$

Substituting the latter relation into Eq. (14) yields, for $a(x)$ for DC's, the basic equation

$$[a(x)-\varpi x]d/dx\ a(x)=(1-\varpi)[a(x)-a_{\rm avnuc}q(x)], \tag{20}$$

where $q(x)$ has yet to be determined, and we note again that Eq. (20) is not exact. Certainly, the choice of DC's simplifies the formulation of the theory, since Eq. (19) applies. However, when comparing against simulation data, it is convenient to have the *flexibility* of using VC's or EC's.

If $q(x)$ is treated as a known quantity, then Eq. (20) has the form of an Abel equation of the second kind.[21] [The same also applies for the $a(x)$ equation for VC's or EC's obtained from Eq. (16) after using Eq. (17) or Eq. (18).] Furthermore, the specific form of these equations allows conversion to an Abel equation of the first kind in terms of the variable $u(x)=[C_{\rm tot}(x)-\varpi x]^{-1}$.[21] For example, from Eq. (20), one obtains

$$du/dx=(2\varpi-1)u^2+(1-\varpi)[a_{\rm avnuc}q(x)-\varpi x]u^3,$$

$$\text{where}\quad u(0)=C_{\rm tot}(0)^{-1}=a(0)^{-1}>0 \tag{21}$$

It follows from Eq. (21) that unless $a_{\rm avnuc}q(x)$ decreases below ϖx, with increasing x (see below), there is a divergence $u\to\infty$, which corresponds to $C_{\rm tot}(x)\to\varpi x$, for *finite* x.

D. Analysis for an exact prescription of nucleation

Here we use simulations to monitor a large number of nucleation events. The cell of each just-nucleated island is constructed, allowing determination of $A_{\rm avnuc}$, and thus $a_{\rm avnuc}$. These cells are also partitioned into subregions overlapping the cells of existing islands of various sizes, allowing a determination of P_s and thus $q(x)$. For the *point-island model*, one has $a(0)\approx0.88$ and $a_{\rm avnuc}\approx0.93$ [cf. Eq. (41)]. Simulation results (thick curves) are shown for $q(x)$ using VC's in Fig. 5(a), and for the corresponding $a(x)$ in Fig. 5(b). In Fig. 5(b), we also show the prediction (thin curve) for $a(x)$ obtained from Eq. (16) with $\varpi=\frac{2}{3}$ using Eq. (18) to relate $C_{\rm tot}(x)$ to $a(x)$, and using the simulated $q(x)$ in Fig. 5(a). Conversely, in Fig. 5(a), we show the prediction (thin curve) for $q(x)$ obtained from Eq. (16) using the simulated $a(x)$ in Fig. 5(b). The predictions of Eq. (16) capture the basic features of the simulation results quite well, given that there still are approximations built into this equation. It should be noted that using Eq. (16) to predict $a(x)$ from specified $q(x)$ can produce a singular behavior for finite x, if $q(x)$ increases ''too quickly.'' This does occur in our calcu-

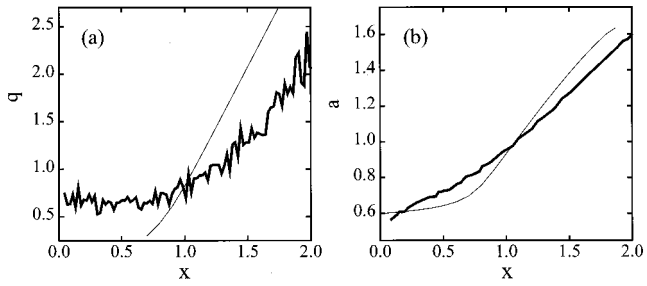

FIG. 6. Simulation results (thick lines) using EC's for the square-island model at 0.1 ML with $h/F=10^7$ for (a) $q(x)$ and (b) the associated $a(x)$. Also shown are predictions obtained from Eq. (16) (thin lines), as described in the text.

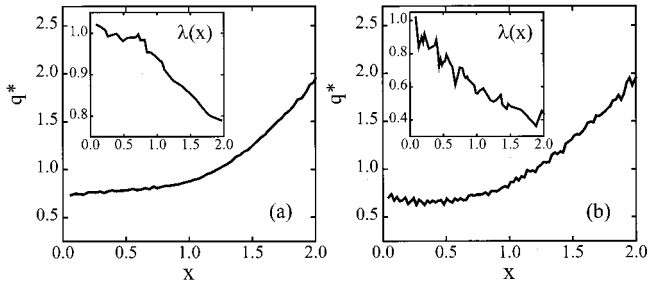

FIG. 7. $q^*(x)$ and $\lambda(x)=a_{\rm nuc}(x)/a(x)$ (insets) for (a) the point-island model, and (b) the square-island model, at 0.1 ML with $h/F=10^7$.

lations, presumably again reflecting approximations in Eq. (16), and our nonasymptotic input $q(x)$. For the *square-island model*,[4] where $a(0)\approx 0.5$ and $a_{\rm avnuc}\approx 0.6$ [cf. Eq. (41)], simulation results (thick curves) are shown for $q(x)$ using EC's in Fig. 6(a), and for the corresponding $a(x)$ in Fig. 6(b). In Fig. 6(b), we also show the predicted $a(x)$ from Eq. (16) with an effective $\varpi=0.87$ using $C_{\rm tot}(x)\approx a(x)$ from Eq. (17), and using the simulated $q(x)$ in Fig. 6(a). Conversely, in Fig. 6(a), we show the predicted $q(x)$ from Eq. (16) using the simulated $a(x)$ in Fig. 6(b). The predictions from Eq. (16) are reasonable for $a(x)$, but not for $q(x)$. The latter no doubt reflects the feature that the simulated $a(x)$ is far from its asymptotic form, and other uncertainties with the use of effective exponents.

E. Further analysis and the ''nucleation-inside-a-cell'' picture

First we introduce a natural factorization of quantities such as P_s and Q_s [or $p(x)$ and $q(x)$]. Let $P_s^*=(N_s/N_{\rm av})Q_s^*$ denote the probability that the cell of the just-nucleated island *overlaps* the cell of some existing island of size s. Then one has the normalization condition $\Sigma_{s>1}P_s^*=M_o$, the mean number of overlapped cells per nucleation event. Let $A_{\rm nuc}(s)$ denote the mean area of the cell of a just-nucleated island which overlaps cells of existing islands of size s. Then we can write

$$A_{\rm avnuc}P_s=A_{\rm avnuc}(N_s/N_{\rm av})Q_s=A_{\rm nuc}(s)(N_s/N_{\rm av})Q_s^* =A_{\rm nuc}(s)P_s^*. \quad (22)$$

Introducing scaling functions $a_{\rm nuc}(x)\approx A_{\rm nuc}(s)/A_{\rm av}$ and $q^*(x)\approx Q_s^*$ (for large $s_{\rm av}$), one has that

$$a_{\rm avnuc}q(x)=a_{\rm nuc}(x)q^*(x), \quad (23)$$

which can be used in Eq. (16). The normalization conditions on P_s^* and P_s imply that $\int_0^\infty dx\, f(x)q^*(x)=M_o$ and $\int_0^\infty dx\, f(x)a_{\rm nuc}(x)q^*(x)=a_{\rm avnuc}$, respectively.

Next we introduce an idealized ''nucleation-inside-a-cell'' picture, providing a simpler interpretation of P_s^* and $A_{\rm nuc}(s)$. It was used in previous work by Mulheran and Robbie (MR),[12] and makes the formalism following in Sec. IV less complex. It involves the simplified view that capture zones or cells of just-nucleated islands always lie entirely within the capture zone or the cell of a single existing island. In this case, P_s^* is just the probability for nucleation within the cell of an island of size s, $M_o=1$, and $A_{\rm nuc}(s)$ is the mean area of the cell of such a nucleated island. Specifically, MR assumed that each nucleation event splits an existing cell in two. This requires that nucleation positions be ''deep within'' cells of existing islands. However, we recognize that it is somewhat unrealistic: nucleation positions tend to be close to the boundaries of capture zones, so that just-nucleated cells typically overlap two or more existing capture zones.[22]

Since nucleation inside a cell does *not* strictly apply, this limits possibilities to test the above ideas. However, for any tessellation of an island distribution, the following analyses are instructive. We determine the probability for nucleation within the cell of an island of size s, and the average area of the cells of such just-nucleated islands, *irrespective* of whether these cells lie entirely within the existing cell of an island of size s. The former might be interpreted as P_s^* and the latter as $A_{\rm nuc}(s)$, although of course these interpretations do *not* precisely match the above descriptions. Nonetheless, from these quantities, we obtain estimates for $q^*(x)$ and $a_{\rm nuc}(x)$ [or $\lambda(x)\equiv a_{\rm nuc}(x)/a(x)$]. Figure 7 shows such $q^*(x)$ and $\lambda(x)$ using VC's for point islands, and EC's for square islands. Corresponding predictions for $a(x)$, using Eq. (23) in Eq. (16), capture the key features of simulation results.

IV. JOINT PROBABILITY DISTRIBUTIONS FOR ISLAND SIZE AND CELL AREA

A. Basic quantities

A particularly significant recent development in nucleation theory was the idea of MR (Ref. 12) to derive rate equations for the joint probability distribution $N_{s,A}$ for the densities of islands of size s atoms, and cell area A (for a suitable tessellation of the island distribution). This quantity is normalized so that $\Sigma_A N_{s,A}=N_s$, with the island densities, N_s defined as above. We shall see that this approach complements the treatment of Sec. III, as the distribution $N_{s,A}$ incorporates the feature that the mean cell area for islands of size s, i.e., $A_s=\Sigma_A A N_{s,A}/N_s$, depends on s in a nontrivial non-mean-field fashion. This approach also supplements or extends that of Sec. III in that the distribution $N_{s,A}$ further-

more incorporates the feature (not explicitly accounted for in Sec. III) that islands of a given size s have cells with a distribution of cell areas A.

Clearly, sources of change for the $N_{s,A}$ include aggregation of diffusing atoms with islands, direct deposition on top of islands, and nucleation. We now deal in a unified fashion with the first two contributions. In the following, the rate at which diffusing atoms aggregate with islands of size s and cell area A is denoted by $\mathbf{R}_{\rm agg}(s,A) \equiv h\sigma_{s,A}N_{s,A}N_1$, defining a dimensionless ''capture number'' $\sigma_{s,A}$. Then, one has $\Sigma_A \sigma_{s,A}N_{s,A} = \sigma_s N_s$. The rate of direct deposition on top of islands of size s is denoted by $\mathbf{R}_{\rm dep}(s,A) \equiv F\kappa_s N_{s,A}$ (where $\kappa_s \approx s$ for compact islands, or $\kappa_s \sim 1$ for point islands). Below, we set $\mathbf{R}_{\rm tot}(s,A) = \mathbf{R}_{\rm agg}(s,A) + \mathbf{R}_{\rm dep}(s,A)$. For *diffusion cells* one has $\sigma_{s,A}/\sigma_{\rm av} = A^f/A^f_{\rm av}$, where $A^f = A - \kappa_s$. If the steady-state condition [Eq. (3)] is recast as $hN_1\sigma_{\rm av}/A^f_{\rm av} = F$, then for DC's it readily follows that

$$\mathbf{R}_{\rm agg}(s,A) = hN_1\sigma_{\rm av}(\sigma/\sigma_{\rm av} = A^f/A^f_{\rm av})N_{s,A} = FA^f N_{s,A}, \quad \text{so} \quad \mathbf{R}_{\rm tot}(s,A) = FAN_{s,A}. \tag{24}$$

Equation (24) applies either for compact or point islands.

The treatment of nucleation terms is more difficult. We introduce the probability $P^*_{s,A}$ that the cell of the just-nucleated islands *overlaps* the cell of an existing island of size s and cell area A. Then, the typical number of cells overlapped per nucleation event is $\Sigma_{s>1}\Sigma_A P^*_{s,A} = M_o$ (cf. Sec. III E). Since this probability should scale with the density $N_{s,A}$, it is natural to decompose:

$$P^*_{s,A} = (N_{s,A}/N_{\rm av})Q^*_{s,A}. \tag{25}$$

We also let $A_{\rm nuc}(s,A)$ denote the average (portion of the) area of the cell for a just-nucleated island which *overlaps* the cell of an existing island of size s and cell area A. Note that $\Sigma_A P^*_{s,A}A_{\rm nuc}(s,A) = A_{\rm nuc}(s)P^*_s$, and that applying $\Sigma_{s>1}$ gives $A_{\rm avnuc}$. For small coverages $\theta \ll 1$, or for point islands, we expect the characteristics of the nucleation process are determined primarily by the geometry of the capture zone tessellation (rather than by the sizes of the small islands within the cells). Thus we expect a *weak* dependence on island size s of $Q^*_{s,A} \approx Q^*_A$ and $A_{\rm nuc}(s,A) \approx A_{\rm nuc}(A)$. We emphasize that cells of just-nucleated islands exhibit a *distribution* of overlap areas, $A_{\rm nuc}$ with cells of existing islands of size s and area A, and that $A_{\rm nuc}(s,A)$ gives only the average. Our formulation does not incorporate the full distribution. Finally, it is also convenient to introduce the probability p_A, that the just-nucleated island has a cell area of A, so $\Sigma_A p_A = 1$ and $\Sigma_A A p_A = A_{\rm avnuc}$.

B. Rate equations for the joint probability distribution

The population $N_{s,A}$, of islands of size s with cells of size A changes primarily for two reasons: (i) Aggregation of diffusing atoms with islands or direct deposition on-top of islands of size $s-1$ (of size s), and cell area A, increases (decreases) $N_{s,A}$. (ii) Nucleation of islands with cells *overlapping* those of existing islands of size s decreases $N_{s,A}$ if the cell area prior to nucleation is A. Nucleation increases

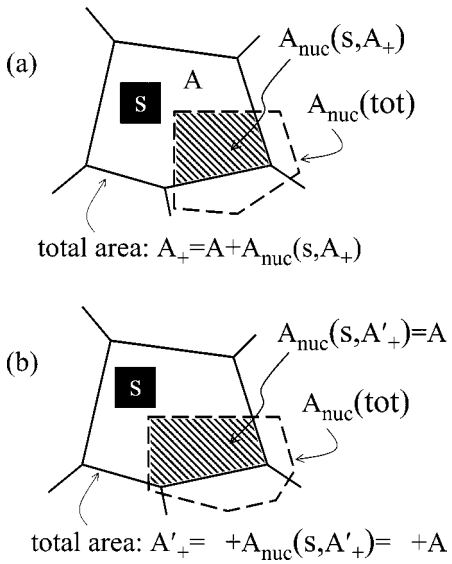

FIG. 8. Schematics for the relation between (a) A_+ and A, and (b) A'_+ and A. Here $A_{\rm nuc}$(tot) denotes the total area of the cell of a just-nucleated island, of which a portion $A_{\rm nuc}(s,\ldots)$ overlaps the cell of the existing island of size s. (This picture is oversimplified for DC's where introducing new cells changes boundaries of existing cells external as well as internal to the new cell.)

$N_{s,A}$ if the cell size prior to nucleation, A_+, is suitably larger than A. In the latter case, the average value of the area A_+ should satisfy $A_+ = A + A_{\rm nuc}(s,A_+)$. See Fig. 8(a). Given a specific functional form for $A_{\rm nuc}$ this relation can be solved to determine a unique functional relationship $A_+ = A_+(s,A)$. See Appendix B. In fact (for a given island size s), there will be a *distribution* of cell areas, A_+, for which nucleation events will create a smaller cell with area A, and $A_+(s,A)$ gives only the average. *Neglecting* this distribution of A_+ values (i.e., utilizing only the average value), we conclude that the rate equations for $N_{s,A}$ have the form

$$d/dt\ N_{s,A} = \mathbf{R}_{\rm tot}(s-1,A) - \mathbf{R}_{\rm tot}(s,A) + \sum^{\#}_{A+} P^*_{s,A+} \times (dN_{av}/dt) - P^*_{s,A}(dN_{\rm av}/dt), \quad \text{for } s>2. \tag{26}$$

The restricted sum $\Sigma^{\#}_{A+}$ is for fixed A, and accounts for the feature that the equation $A_+ = A + A_{\rm nuc}(s,A_+)$ can have more than one solution A_+ for fixed A (i.e., a cell of size A can be created by nucleation within a larger cell sometimes with more than one size A_+ after removal of an area $A_{\rm nuc}$.) In the scaling regime, this restricted sum may be replaced by a factor dA_+/dA. Perhaps the simplest scenario is that $A_{\rm nuc}(s,A_+) = A_{\rm nuc}(A_+) = \mu A_+$ (where we expect that $\mu M_o < 1$), so $A_+(A) = A/(1-\mu)$, and $dA_+/dA = 1/(1-\mu)$. It is necessary to develop a separate equation for $N_{2,A}$, which provides a ''boundary condition'' on the above coupled set of equations. One has that

$$d/dt\ N_{2,A} = -\mathbf{R}_{\rm tot}(2,A) + p_A(dN_{\rm av}/dt). \tag{27}$$

The above equations (26) and (27) no longer suffer from the approximation implicit in Eq. (12) of neglecting the distribution of cell areas for each island size. However, they do not account for changes in cell areas due to growth of the island within the cell and of neighboring islands, leading to slight shifts in cell boundaries.[18] Again, we anticipate that the net effect is small.

C. Quasihydrodynamic scaling analysis

Again, our interest is in the scaling regime of large s_{av} and A_{av}, so we introduce the natural scaling variables $x=s/s_{av}$ and $\alpha=A/A_{av}$, and the appropriate scaling function $\mathbf{F}$, defined by

$$N_{s,A}\approx N_{av}(s_{av}A_{av})^{-1}\mathbf{F}(x,\alpha,\theta)=\theta^2(s_{av})^{-3}\mathbf{F}(x,\alpha,\theta), \tag{28}$$

where $\int_0^\infty d\alpha\,\mathbf{F}(x,\alpha,\theta)=f(x,\theta)$ and $\int_0^\infty d\alpha\,\alpha\mathbf{F}(x,\alpha,\theta)=a(x,\theta)f(x,\theta)$. Defining the average $\langle\cdot\rangle=(\int_0^\infty d\alpha\,\mathbf{F})^{-1}(\int_0^\infty d\alpha\,\mathbf{F}\cdot)=f^{-1}(\int_0^\infty d\alpha\,\mathbf{F}\cdot)$, then these conditions correspond to $\langle 1\rangle=1$ and $\langle\alpha\rangle=a(x)$. To proceed further, we introduce a scaling function for $\sigma_{s,A}/\sigma_{av}\approx\mathbf{C}_{agg}(x,\alpha,\theta)$, and set

$$\mathbf{C}_{tot}(x,\alpha,\theta)=(1-\theta)\mathbf{C}_{agg}(x,\alpha,\theta)+\theta\;x \quad \text{for compact islands,}$$

and

$$\mathbf{C}_{tot}=\mathbf{C}_{agg} \quad \text{for point islands.} \tag{29}$$

Then one has $\int_0^\infty d\alpha\,\mathbf{C}_{tot}(x,\alpha,\theta)\mathbf{F}(x,\alpha,\theta)=C_{agg}(x,\theta)f(x,\theta)$ and $\mathbf{C}_{tot}(x,\alpha,\theta)=\alpha$ for DC's. We also set $Q^*_{s,A}\approx\mathbf{q}^*(x,\alpha,\theta)$, so that $\int_0^\infty dx\int_0^\infty d\alpha\mathbf{F}(x,\alpha,\theta)\times\mathbf{q}^*(x,\alpha,\theta)=M_o$, which follows from the normalization condition on $P^*_{s,A}$. We also introduce scaling functions describing

$$A_{nuc}(s,A)/A_{av}\approx\alpha_{nuc}(x,\alpha,\theta),$$

$$A_+(s,A)/A_{av}\approx\alpha_+(x,\alpha,\theta),$$

$$p_A\approx(A_{av})^{-1}\mathbf{p}(\alpha,\theta), \tag{30}$$

which satisfy the normalization conditions that $\int_0^\infty dx\int_0^\infty d\alpha\,\alpha_{nuc}(x,\alpha)\mathbf{q}^*(x,\alpha)\mathbf{F}(x,\alpha)=a_{avnuc}$, and $\int_0^\infty d\alpha\,\mathbf{p}(\alpha,\theta)=1$. Note that if $A_{nuc}(s,A)=A_{nuc}(A)=\mu A$, then one has $\alpha_{nuc}(x,\alpha,\theta)=\mu\alpha$ and $A_+(A)=A/(1-\mu)$, so $\alpha_+(x,\alpha,\theta)=\alpha/(1-\mu)$. Appendix C provide a discussion of the relationship between these scaling functions and the reduced functions, $q^*(x)$ and $a_{nuc}(x)$, introduced in Sec. III.

Analyzing the various terms in the rate equations (26) in the scaling limit, one has

$$d/dt\;N_{s,A}\approx\theta F(s_{av})^{-3}[(2-3\varpi)\mathbf{F}-\varpi x\partial/\partial x\mathbf{F}+(1-\varpi)\alpha\partial/\partial\alpha\mathbf{F}+\theta\partial/\partial\theta\mathbf{F}],$$

$$\mathbf{R}_{tot}(s-1,A)-\mathbf{R}_{tot}(s,A)\approx-\partial/\partial s\mathbf{R}_{tot}(s,A)\approx-\theta F(s_{av})^{-3}\partial/\partial x(\mathbf{C}_{tot}\mathbf{F}), \tag{31}$$

$$P^*_{s,A}(dN_{av}/dt)\approx\theta F(s_{av})^{-3}(1-\varpi)\mathbf{q}^*\mathbf{F},$$

$$\sum_{A^+}^{\#}P^*_{s,A^+}(dN_{av}/dt)\approx\theta F(s_{av})^{-3}(1-\varpi)\times\mathbf{q}^*(x,\alpha_+,\theta)\mathbf{F}(x,\alpha_+,\theta)d\alpha_+/d\alpha,$$

where the arguments of $\mathbf{F}$ and $\mathbf{q}^*$ are (x,α,θ), unless otherwise indicated. Substituting these results into Eq. (26) yields the PDE

$$\begin{aligned}(2-3\varpi)\mathbf{F}(x,\alpha,\theta)&-\varpi x\partial/\partial x\mathbf{F}(x,\alpha,\theta)\\&+(1-\varpi)\alpha\partial/\partial\alpha\mathbf{F}(x,\alpha,\theta)+\theta\partial/\partial\theta\mathbf{F}(x,\alpha,\theta)\\&=-\partial/\partial x[\mathbf{C}_{tot}(x,\alpha,\theta)\mathbf{F}(x,\alpha,\theta)]\\&\quad+(1-\varpi)\mathbf{q}^*(x,\alpha_+,\theta)\mathbf{F}(x,\alpha_+,\theta)d\alpha_+/d\alpha\\&\quad-(1-\varpi)\mathbf{q}^*(x,\alpha,\theta)\mathbf{F}(x,\alpha,\theta).\end{aligned} \tag{32}$$

The terms on the LHS of Eq. (32) come from $d/dt\;N_{s,A}$. The first term on the RHS describes island growth (by both aggregation and direct on-top deposition), and the last two terms on the RHS describe gain and loss by nucleation, respectively. We note again that if $A_{nuc}(s,A)=\mu A$, then one has $\alpha_+=\alpha/(1-\mu)$ and $d\alpha_+/d\alpha=1/(1-\mu)$. Equation (32) generalizes the PDE obtained by MR[12] in the following ways: (i) it is not restricted to the idealized and unphysical ''nucleation within a cell'' picture (cf. Secs. III E and IV E), and allows for general functional forms for Q^* and A_{nuc} (and their scaling functions); (ii) it applies for any tessellation (i.e., not just DC's); and (iii) it allows for an explicit θ dependence. The first generalization is of fundamental importance for a physically realistic formulation, and the second is of practical value. We also emphasize that it is *approximate*, as it neglects fluctuations in A_+ areas (cf. Sec. IV C).

A similar analysis of Eq. (27) reveals that the terms on the RHS dominate those on the LHS by a factor of s_{av}. Setting the scaled form of the RHS terms to zero yields the ''boundary condition''

$$\mathbf{C}_{tot}(0,\alpha,\theta)\mathbf{F}(0,\alpha,\theta)=(1-\varpi)\mathbf{p}(\alpha,\theta), \tag{33}$$

which refines and simplifies MR's result.[12] The term on the LHS corresponds to the loss of dimers with cells of scaled area α due to island growth, and the term on the RHS to gain due to nucleation. A key constraint following from this relation will be discussed in Sec. IV E.

D. Moment analysis of the PDE for F: relation to previous ODE's

In this section, we assume that *θ-independent scaling* applies (but see Appendix C), although some of the analysis can be straightforwardly extended to the more general case where additional $\theta\partial/\partial\theta$ terms appear. One might analyze Eq. (32) by either integrating with respect to x, or with respect to α. The former analysis is presented in Appendix D. The latter is presented below. More specifically, the general strategy is to apply the operation $\int_0^\infty\alpha^n d\alpha\cdot$ to Eq. (32), performing integration of parts on the $\alpha\partial/\partial\alpha\mathbf{F}$ term, together with suit-

able rearrangements of the resulting equations to obtain ODE's for various moments of **F**. We will also use the identities

$$\int_0^\infty d\alpha\ \mathbf{F}=f,\quad \int_0^\infty d\alpha\ \alpha\mathbf{F}=af,\quad \int_0^\infty d\alpha\ \alpha^2\mathbf{F}=a^2f+\sigma^2 f,$$

$$\int_0^\infty d\alpha\ \alpha^3\mathbf{F}=a^3f+3a\sigma^3 f+\kappa f,\ldots \tag{34}$$

where $a=\langle\alpha\rangle$, $\sigma^2(x)=\langle(\alpha-\langle\alpha\rangle)^2\rangle$, $\kappa(x)=\langle(\alpha-\langle\alpha\rangle)^3\rangle,\ldots$, are the mean, variance, skewness, . . . , respectively, of the scaled cell area distribution (for a given scaled island size, x). Below we present an analysis for the moments with $n=0$, 1, and 2.

(i) *Zeroth moment* ($n=0$): Applying $\int_0^\infty d\alpha\cdot$ to Eq. (32), one immediately recovers exactly the fundamental equation (5) for the scaling function $f(x)$ describing the island size distribution:

$$(1-2\varpi)f(x)-\varpi x d/dx\ f(x)=-d/dx[C_{\rm tot}(x)f(x)]. \tag{35}$$

Note that the nucleation terms exactly cancel under this procedure.

(ii) *First moment* ($n=1$): First we comment on the result of applying $\int_0^\infty \alpha\ d\alpha\cdot$ to the nucleation terms in Eq. (32). If α_+^I denotes the inverse function to $\alpha_+=\alpha_+(x,\alpha)$, i.e., $\alpha=\alpha_+^I(x,\alpha_+)$, then one has that

$$\begin{aligned}\int_0^\infty d\alpha\ \alpha[\mathbf{q}^*(x,\alpha)\mathbf{F}(x,\alpha)-\mathbf{q}^*(x,\alpha_+)\mathbf{F}(x,\alpha_+)d\alpha_+/d\alpha]&\\ =\int_0^\infty d\alpha[\alpha-\boldsymbol{\alpha}_+^I(x,\alpha)]\mathbf{q}^*(x,\alpha)\mathbf{F}(x,\alpha)&\\ =\int_0^\infty d\alpha\ \alpha_{\rm nuc}(x,\alpha)\mathbf{q}^*(x,\alpha)\mathbf{F}(x,\alpha)&\\ =a_{\rm nuc}(x)q^*(x)f(x),&\end{aligned} \tag{36}$$

using the identity $\alpha-\alpha_+^I(x,\alpha)=\alpha_{\rm nuc}(x,\alpha)$ from Appendix *B*, and the relation for $a_{\rm nuc}(x)$ in Appendix *C*. Thus, applying $\int_0^\infty \alpha\ d\alpha\cdot$ to Eq. (32) yields

$$\begin{aligned}\varpi d/dx(xaf)&=d/dx(aC_{\rm tot}\,f)\\ &\quad+d/dx\left[\int_0^\infty d\alpha[\alpha-a(x)]\mathbf{C}_{\rm tot}(x,\alpha)\mathbf{F}(x,\alpha)\right]\\ &\quad+(1-\varpi)a_{\rm nuc}(x)q^*(x)f(x),\end{aligned} \tag{37}$$

refining Eq. (15) by introducing an extra term which scales with the variance σ^2. This leads to an important correction of Eq. (16) by accounting for the distribution of cell areas for each island size.

Further reduction of Eq. (37) is achieved conveniently by assuming that $\mathbf{C}_{\rm tot}(x,\alpha)=\gamma\alpha+(1-\gamma)$, which is consistent with $C_{\rm tot}(x)=\gamma a(x)+(1-\gamma)$, so then the integral in Eq. (37) reduces to $\gamma\sigma^2(x)f(x)$. This relationship applies exactly for diffusion cells, where $\gamma=1$ (and we assume it holds approximately for point islands and VC's where $\gamma\approx0.7$, or for square islands and EC's at around 0.1 ML, where $\gamma\approx1$). One can use Eq. (5) or (35) to reduce Eq. (37) to an equation analogous to Eq. (16), i.e.

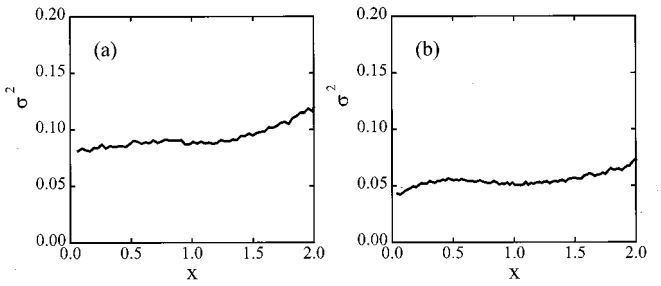

FIG. 9. Simulation results for σ^2 vs x for (a) the point-island model using VC's, and (b) the square-island model using EC's, at 0.1 ML with $h/F=10^7$.

$$\begin{aligned}[C_{\rm tot}(x)-\varpi x]d/dx\ a(x)&=(1-\varpi)[a(x)-a_{\rm nuc}(x)q^*(x)]\\ &\quad-\gamma d/dx(\sigma^2 f)/f.\end{aligned} \tag{38}$$

Using Eq. (5) or Eq. (35) again to completely eliminate f yields

$$\begin{aligned}[(C_{\rm tot}-\varpi x)-\gamma^2\sigma^2(C_{\rm tot}-\varpi x)^{-1}]da/dx+\gamma d/dx(\sigma^2)&\\ =(1-\varpi)[a-a_{\rm nuc}q^*]-\gamma(2\varpi-1)\sigma^2(C_{\rm tot}-\varpi x)^{-1}.&\end{aligned} \tag{39}$$

This equation can be integrated for $a(x)$ given information on σ^2 (and $a_{\rm nuc}$ and q^*). An alternative strategy is to obtain a second equation involving σ^2 (see below).

(iii) *Second moment* ($n=2$): Next, we apply $\int_0^\infty \alpha^2 d\alpha\cdot$ to Eq. (32). For simplicity, we discuss only on the case where $\mathbf{C}_{\rm tot}(x,\alpha)=\alpha$ (e.g., tessellations based on DC's). Then, after some manipulation, one obtains

$$\begin{aligned}(1+\varpi x\partial/\partial x)(a^2f+\sigma^2 f)&\\ =\partial/\partial x(a^3f+3a\sigma^2 f+\kappa f)+(1-\varpi)&\\ \times\int_0^\infty d\alpha\ \alpha_{\rm nuc}(x,\alpha)[2\alpha-\alpha_{\rm nuc}(x,\alpha)]&\\ \times\mathbf{q}^*(x,\alpha)\mathbf{F}(x,\alpha).&\end{aligned} \tag{40}$$

To close this equation together with Eq. (38), one might set the third-order cumulant to zero (i.e., $\kappa\approx0$), as well as higher-order cumulants, of the cell area distribution. See Appendix E.

E. Analysis and further constraints from moment equations [or from Eq. (33)]

The simplest strategy for an analysis of Eq. (39) is motivated by simulation results, indicating that σ^2 is roughly independent of x [so $d/dx(\sigma^2)\approx0$]. This applies for either point islands using VC's, or square islands using EC's, as shown in Fig. 9. Our goal here is to obtain some insight into the effect of constant $\sigma^2>0$, for the case of point islands

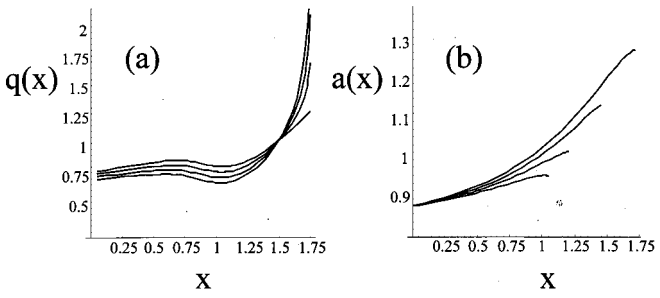

FIG. 10. (a) $q(x)$ for point islands for various choices of fixed $\sigma^2>0$ predicted from Eq. (39) taking simulation results for $a(x)$ from Fig. 5(b) as input. (b) $a(x)$ for point islands various choices of fixed $\sigma^2>0$ predicted from Eq. (39), after replacing $a_{\rm nuc}q^*$ with $a_{\rm avnuc}q$, taking simulation results for $q(x)$ from Fig. 5(a). Specifically, we choose $\sigma^2=0.0$, 0.03, 0.06, and 0.09 (curves from top to bottom at $x=1$). Other parameters are described in the text.

where $\varpi=2/3$ and $\gamma\approx 0.7$. *First*, we have taken simulation results for $a(x)$ from Fig. 5(b) as input to Eq. (39), and extracted corresponding $a(x)$ for various choices of fixed $\sigma^2>0$. Results shown in Fig. 10(a) indicate some improvement in the match to simulation $a(x)$ increasing $\sigma^2>0$. *Second*, we take simulation results for $q(x)$ from Fig. 5(a), and integrated Eq. (39) for $a(x)$, after replacing $a_{\rm nuc}q^*$ with $a_{\rm avnuc}q$. Results shown in Fig. 10(b) indicate that the increase of $a(x)$ with x is reduced with increasing σ^2, a feature which improves the agreement with simulation results shown in Fig. 5(b). However, the singular behavior mentioned in Sec. III D due to $q(x)$ increasing ''too rapidly'' becomes problematic for larger σ^2, limiting the range of integrability. This must reflect inadequacies in Eq. (38), and our nonasymptotic input $q(x)$.

Next we comment on some significant constraints following from the moment equations in Sec. IV D. First applying $\int_0^\infty dx\cdot$ to Eq. (35) readily recovers the identity [Eq. (10a)] that $C_{\rm tot}(0)f(0)=1-\varpi$. Second, applying $\int_0^\infty dx\cdot$ to Eq. (37), one obtains

$$(1-\varpi)[a_{\rm avnuc}-a(0)]=\int_0^\infty d\alpha[\alpha-a(0)]\mathbf{C}_{\rm tot}(0,\alpha)\mathbf{F}(0,\alpha)$$
$$=\gamma\sigma^2(0)f(0), \qquad (41)$$

where the last equality assumes again that $\mathbf{C}_{\rm tot}(x,\alpha)=\gamma\alpha+(1-\gamma)$. To obtain Eq. (41), we also use a relation for $a_{\rm avnuc}$ in Appendix C, and the identity $C_{\rm tot}(0)f(0)=1-\varpi$. Since $\sigma^2>0$, Eq. (41) implies that $a_{\rm avnuc}>a(0)$ (contrasting Sec. III). The inequality is reasonable, since not all dimers are ''just nucleated,'' and those nucleated earlier should typically have smaller cell areas. However, since $\sigma^2\ll 1$ (see Fig. 9), one finds that $a_{\rm avnuc}$ is quite close to $a(0)$. Third, we note that applying $\int_0^\infty dx\cdot$ to Eq. (40) does not yield a simple constraint, unlike for the lower order equations.

Finally, it is instructive to note that one can perform a moment analysis of the boundary condition [Eq. (33)], which in fact has the advantage of clarifying the significance of this somewhat obscure constraint. Applying to Eq. (33) the operation $\int_0^\infty d\alpha\cdot$ recovers the key result [Eq. (10a)], which was also obtained by applying $\int_0^\infty dx\cdot$ to the ODE [Eq. (35)]. Applying to Eq. (33) the operation $\int_0^\infty \alpha\, d\alpha\cdot$ recovers relation (41),[23] which was also obtained by applying $\int_0^\infty dx\cdot$ to the ODE [Eq. (37)].

F. Formulation for the ''nucleation-inside-a-cell'' picture

To make a closer connection with the formulation of MR,[12] we follow Sec. III E and restrict our consideration to the somewhat artificial ''nucleation-inside-a-cell'' picture. Again, we emphasize that this picture is somewhat unrealistic. Here $P^*_{s,A}=(N_{s,A}/N_{\rm av})Q^*_{s,A}$ simply becomes the probability for nucleation within the cell of an island of size s and cell area A, where $\Sigma_{s>1}\Sigma_A\ P^*_{s,A}=M_o=1$. Also, $A_{\rm nuc}(s,A)$ now denotes the average area of the (entire) cell for an island which is just-nucleated inside a cell of area A belonging to an existing island of size s. To provide some specific examples, MR (Ref. 12) suggested that $P^*_{s,A}\propto A^4$, for irreversible island formation. The idea is that the probability of finding a diffusing atom in a cell should scale like A^2 (the probability for deposition in the cell $\sim A$ *times* the lifetime $\sim A$), and two such atoms are required for nucleation. MR also suggested that $A_{\rm nuc}(s,A)=\lambda A$, where they regarded $\lambda<1$ as a fitting parameter (roughly corresponding to μM_o in Sec. IV B), and chose $\lambda\approx 0.4$. However, for a realistic description of nucleation, we expect that at least λ should decrease with increasing s (cf. Fig. 7), i.e. for increasing $A_s/A_{\rm av}$.

For the nucleation-within-a-cell picture, the derivation of the rate equations for $N_{s,A}$, and the scaling equation for $\mathbf{F}(x,\alpha)$ is unchanged from the more general presentation above. To make a direct comparison with the analysis of MR, note that if $A_{\rm nuc}(s,A)=\lambda A$, then one has $A_+(A)=A/(1-\lambda)$ and $dA_+/dA=1/(1-\lambda)$, which implies that $\alpha_+=\alpha/(1-\lambda)$ and $d\alpha_+/d\alpha=1/(1-\lambda)$. If $P^*_{s,A}\propto A^4$, then one also has that $\mathbf{q}^*(x,\alpha)\propto\alpha^4$. Using these results in Eq. (32) recovers the MR form.

Finally, we discuss the form of the boundary condition [Eq. (27)], and specifically p_A, for the 'nucleation-in-a-cell' picture. As shown schematically in Fig. 8(b), islands of size 2 with cell area A are obtained by nucleation in cells of existing islands with larger area A'_+ where on average $A_{\rm nuc}(s,A'_+)=A_{\rm nuc}({\rm tot})=A$. This relation can be solved to determine a unique functional relationship $A'_+=A'_+(s,A)$. See Appendix B. *Neglecting* the distribution of A'_+ values, it follows that

$$p_A=\sum_{s>2}\ \sum^{\#}_{A'+}\ P^*_{s,A'+}. \qquad (42)$$

The restricted sum $\Sigma^{\#}_{A*+}$ is for fixed A, and accounts for the feature that the equation $A_{\rm nuc}(s,A'_+)=A$ can have more than one solution A'_+ for fixed A. In the scaling limit, this restricted sum may be replaced by a factor dA'_+/dA. The MR proposal implies that $A_{\rm nuc}(A'_+)=\lambda A'_+$, so $A'_+(A)=A/\lambda$, and $dA'_+/dA=1/\lambda$. Introducing a scaling function describing

$A'_+(s,A)/A_{av} \approx \alpha'_+(x,\alpha)$, one has $\alpha'_+ = \alpha/\lambda$ and $d\alpha'_+/d\alpha = 1/\lambda$ for the MR proposal. The RHS of Eq. (33) can be rewritten to give the relation

$$\mathbf{C}_{tot}(0,\alpha,\theta)\mathbf{F}(0,\alpha,\theta) = (1-\varpi)\int_0^\infty dx\ \mathbf{q}^*(x,\alpha'_+,\theta) \times \mathbf{F}(x,\alpha'_+,\theta)d\alpha'_+/d\alpha, \qquad (43)$$

which can be directly compared with MR's ''boundary condition'' equation[12] [after using $\mathbf{q}^*(x,\alpha) \propto \alpha^4$], and which refines and simplifies their result.

V. CONCLUSIONS AND FUTURE DIRECTIONS

In this paper, we have provided a theoretical analysis for the non-mean-field dependence of adatom capture on island size, noting that this dependence is of central importance as it controls the shape of the island size distribution. We first developed an analysis based on rate equations for the capture zone areas,[11] and demonstrated the success of its predictions for an exact prescription of nucleation. We also extend the analysis by Mulheran and Robbie[12] for the joint probability distribution function for island sizes and cell areas. A moment analysis of equations for this joint distribution is shown to recover those above from a direct analysis of capture zone areas, with some refinements accounting for the distribution of cell areas for each island size. The key quantities in this formalism are scaling functions for the island size distribution, $f(x)$, and capture zone areas, $a(x)$, and the variance of the cell area distribution, $\sigma^2(x)$, as functions of the scaled island size x. These and many other scaling functions introduced in this work, and the basic relations satisfied by and between them, can be tested in simulations for both point and compact islands. However, since the main focus of this paper was on the development of an analytical theory for nucleation, comprehensive simulation results will be presented elsewhere.

An important success of our analysis is that it does in fact produce a strong non-mean-field correlation between island size and cell area, that was first discovered in simulations,[7] and later in experimental data.[8,9] We note that visual inspection of the form of $\mathbf{F}(x,\alpha)$ in the numerical study of MR (Ref. 12) shows that it also recovers this strong correlation. As an aside, it is appropriate to note that scatter plots for σ_s/σ_{av} versus s/s_{av} obtained from our previous analyses of experimental data[8,9] in fact constitute crude versions of $\mathbf{F}$ plots consistent with the numerical analysis of MR. From these scatter plots, one can even estimate the variance of the cell area distribution, $\sigma^2(x)$, the quantity considered in Sec. IV D and in Appendix E. Other recent work[24] used a level set approach to analyze adatom capture beyond the mean-field treatment, thus providing an accurate island size distribution when incorporated into the rate equations (in the spirit of Refs. 7–9). However, this study considered only a ''relatively small'' range of $h/F = 10^5 - 10^7$ (and a broad range of coverages up to 0.2 ML), rather than examining the scaling limit via a quasihydrodynamic analysis as here and in Refs. 7–9. As a result, it seems that the observed quasilinear $\sigma_s \approx as+b$ (Ref. 24) are strongly influenced by nonasymptotic effects, and by the inhibition of nucleation for higher coverages. (Indeed, our analyses reveal a more linear behavior for higher coverages.) Such a simple linear form for σ_s would not emerge exactly from the type of theories developed here or by MR.

Finally, we note again that our analyses use data from simulations characterizing nucleation as input to rate equations. A self-contained analysis requires some hypotheses about the functions characterizing nucleation (as in the MR analysis of the joint probability distribution which invokes various such assumptions within the framework of a simplified nucleation-inside-a-cell picture). Utilizing both experimental data and simulations,[22] we have characterized nucleation positions, and find that these typically occur close to the boundaries of capture zones. Thus cells of just-nucleated islands typically overlap more than one cell of an existing island. We shall present details of these observations, and of a corresponding refined theoretical analysis, in a separate paper.

ACKNOWLEDGMENTS

J.W.E. was supported for this work by NSF Grant Nos. EEC-0085604 and CHE-0078596. His research was performed at Ames Laboratory, which is operated for the U.S. Department of Energy (U.S. DOE) by Iowa State University under Contract No. W-7405-Eng-82. M.C.B. was supported by the U.S. DOE at Lawrence Livermore National Laboratory which is operated for the U.S. DOE by the University of California, under Contract No. W-7405-ENG-48.

APPENDIX A: SHORT-TIME EXPANSIONS

It is instructive to use rate equations to examine transient behavior for *very short times* before the steady-state regime is established. Since here $\theta \ll 1$, we can ignore direct deposition terms. Using $N_1 \approx Ft = \theta$ from Eq. (2), and $d/dt\ N_{s>l} \approx R_{agg}(s-1)$ from Eq. (1) after neglecting the higher-order $R_{agg}(s)$ term, we obtain

$$N_s \approx (\sigma_1\sigma_2\ldots\sigma_{s-1})(h/F)^{s-1}\theta^{2s-1}/(2s-1)!!. \qquad (A1)$$

Analyses of cell or capture zone areas is more complicated. Note that for short times, the above shows that most islands have $s=2$, so that $N_2 \approx N_{av}$, $A_2N_2 \approx 1$, and $A_2 \approx A_{av} = (N_{av})^{-1}$. Below we consider only the 'nucleation-inside-a-cell' picture, and adopt a MR-type choice of $A_{nuc}(s) = \lambda A_s$, with $\lambda < 1$ (cf Sec. III E), so initially $A_{avnuc} = \Sigma_{s>1} A_{nuc}(s)N_s/N_{av} < (N_{av})^{-1} \approx A_2$. Then, using $A_{avnuc}P_s = = A_{nuc}(s)(N_s/N_{av})Q_s^*$, and $(N_{av})^{-1}dN_{av}/dt \approx 3F(Ft)^{-1}$, we have, from Eq. (12), that

$$d/dt(A_2N_2) \approx -A_2R_{agg}(2) + A_{avnuc}P_3(dN_{av}/dt) \approx -h\sigma_2(Ft) + 3\lambda F(Ft)^{-1}(A_3N_3)Q_3^* \qquad (A2)$$

and

$$d/dt(A_sN_s) \approx A_{s-1}R_{agg}(s-1) - A_{avnuc}P_s(dN_{av}/dt)$$
$$\approx h\sigma_{s-1}(Ft)(A_{s-1}N_{s-1})$$
$$-3\lambda F(Ft)^{-1}(A_sN_s)Q_s^* \quad \text{(A3)}$$

for $s>2$. In the A_2N_2 equation, there are no loss terms from nucleation, and we have dropped the nucleation terms for $s>3$ which are negligible compared with the $s=3$ term. To analyze these equations, we choose $Q_s^*=c_n(A_s/A_{av})^n$, extending the theory of MR, where c_n is determined by normalization, so $c_0=c_1=1$. We look for solutions to Eqs. (A2) and (A3) of the form

$$A_2N_2 \approx 1-\kappa_2\sigma_2(h/F)\theta^2$$

$$\text{and} \quad A_sN_s \approx \kappa_s(\sigma_2\sigma_3\ldots\sigma_{s-1}) \times (h/F)^{s-2}\theta^{2s-4} \quad \text{for } s>2, \quad \text{(A4)}$$

$$\text{so } A_2/A_{av}\approx 1 \text{ and } A_s/A_{av}\approx 5\times 7\times\cdots\times(2s-1)\kappa_s, \text{ for } s>2.$$

Then, the coefficients c_s satisfy[25]

$$-2\kappa_2 = -1+3(5)^n\lambda c_n(\kappa_3)^{n+1},$$
$$2\kappa_3 = 1-3(5)^n\lambda c_n(\kappa_3)^{n+1},$$
$$4\kappa_4 = \kappa_3-3(5\times 7)^n\lambda c_n(\kappa_4)^{n+1},\ldots. \quad \text{(A5)}$$

Solving these equations for $s>2$ reveals that, for any n,[26]

$$\kappa_s \to 1/[2\times 4\times 6\times\cdots\times(2s-4)],$$

$$\text{so } A_s/A_{av}\to[(2s-1)/(2s-4)](A_{s-1}/A_{av}), \quad \text{as } \lambda c_n\to 0 \quad \text{(A6a)}$$

and

$$\kappa_s \to 1/[5\times 7\times 9\times\cdots\times(2s-1)]$$
$$\text{so } A_s/A_{av}\to 1 \quad \text{as } \lambda c_n\to 1. \quad \text{(A6b)}$$

Thus, for realistic λ, one expects that A_s/A_{av} increases with s in the early stages of deposition. This reflects the feature that larger islands were typically created earlier and with larger capture zones.[7]

APPENDIX B: RELATIONS INVOLVING A_{nuc}

The relation $A_+=A+A_{nuc}(s,A_+)$, shown schematically in Fig. 8(a), applies for general A and $A_+=A(s,A)$. Thus, upon replacing A_+ by A, and consistently replacing A by $A-A_{nuc}(s,A)$, one obtains the identity $A_+[s,A-A_{nuc}(s,A)]=A$. Analogously, one can write

$$\alpha_+=\alpha+\alpha_{nuc}(x,\alpha_+) \text{ and thus } \alpha_+[x,\alpha-\alpha_{nuc}(x,\alpha)]=\alpha. \quad \text{(B1)}$$

Then using our definition of the inverse function α_+^I, it follows that

$$\alpha-\alpha_{nuc}[x,\alpha]=\alpha_+^I(x,\alpha), \text{ or } \alpha_{nuc}(x,\alpha)=\alpha-\alpha_+^I(x,\alpha). \quad \text{(B2)}$$

These results can be readily checked for the choice $A_{nuc}(s,A)=\mu A$, where $\alpha_+(\alpha)=\alpha/(1-\mu)$, so $\alpha_+^I(\alpha)=(1-\mu)\alpha$, and $\alpha-\alpha_+^I(\alpha)=\mu\alpha$.

The relation $A=A_{nuc}(s,A'_+)$ also applies for general A and $A'_+(s,A)$. See Fig. 8(b). Thus one can also write $\alpha=\alpha_{nuc}(x,\alpha'_+(x,\alpha))$. If α'^I_+ denotes the inverse function of $\alpha'_+=\alpha'_+(x,\alpha)$, then one has

$$\alpha=\alpha'^I_+(x,\alpha'_+) \quad \text{so} \quad \alpha'^I_+=\alpha_{nuc}. \quad \text{(B3)}$$

For the choice $A_{nuc}(s,A)=\mu A$, one has $\alpha'_+(\alpha)=\alpha/\mu$, so $\alpha'^I_+(\alpha)=\alpha_{nuc}(\alpha)=\mu\alpha$.

APPENDIX C: MR-TYPE FORMS OF SCALING FUNCTIONS FOR Q^* AND A_{nuc}

First we consider quantities which reflect the probability for nucleation overlapping a cell. For $Q^*_{s,A}\approx\mathbf{q}^*(x,\alpha)$, we have that $\int_0^\infty d\alpha\ \mathbf{q}^*(x,\alpha)\mathbf{F}(x,\alpha)=q^*(x)f(x)$, where $\int_0^\infty dx\ f(x)q^*(x)=M_o$. MR (Ref. 12) suggested that the probability of nucleation within a specific cell scales like A^4, for irreversible island formation, where A is the area of that cell, so we write $\mathbf{q}^*\approx c\alpha^4$. Then, one has

$$q^*(x)=c\int_0^\infty d\alpha\ \alpha^4\mathbf{F}(x,\alpha)/f(x)=ca(x)^4+(\text{corrections}). \quad \text{(C1)}$$

The corrections reflect the finite width of the cell area distribution for a specific scaled island size x (cf. Sec. IV D). Our data for $q^*(x)$ does show an increase with x significantly greater than that for $a(x)$:$q^*(2)/q^*(0)=3.5$ versus $a(2)/a(0)=1.5$ for point islands, and $q^*(2)/q^*(0.5)=3.6$ versus $a(2)/a(0.5)=2.8$ for square islands. However, the precise relation between $q^*(x)$ and $a(x)$ cannot be simple [e.g., for compact islands, $q^*(x)$ decreases, whereas $a(x)$ increases for small x]. For the nucleation-within-a-cell picture, we estimate that $c\approx 0.64$ from a fit to our point island data, and using the condition that $\int_0^\infty d\alpha\ \mathbf{q}^*(\alpha)g(\alpha)=M_o=1$. Here, we denote the total cell area distribution (cf. Appendix D) as $g(\alpha)=\int_0^\infty dx\ \mathbf{F}(x,\alpha)$.

Next we consider quantities describing the area of cells of just-nucleated islands. For $A_{nuc}(s,A)/A_{av}\approx\alpha_{nuc}(x,\alpha)$, we have $\int_0^\infty d\alpha\ \alpha_{nuc}(x,\alpha)\mathbf{q}^*(x,\alpha)\mathbf{F}(x,\alpha)=a_{nuc}(x)q^*(x)f(x)$, where $a_{avnuc}=\int_0^\infty dx\ a_{nuc}(x)q^*(x)f(x)$. If $A_{nuc}(s,A)=\mu A$, so $\alpha_{nuc}(x,\alpha)=\mu\alpha$; then it follows that

$$a_{nuc}(x)=\mu\int_0^\infty d\alpha\ \alpha\mathbf{q}^*(x,\alpha)\mathbf{F}(x,\alpha)/q^*(x)f(x) \quad \text{and}$$

$$a_{avnuc}=\mu\int_0^\infty dx\int_0^\infty d\alpha\ \alpha\mathbf{q}^*(x,\alpha)\mathbf{F}(x,\alpha). \quad \text{(C2)}$$

Thus since $\int_0^\infty dx\int_0^\infty d\alpha\ \alpha\mathbf{F}(x,\alpha)=1$, one expects that a_{avnuc} is similar to (but not exactly equal to) μM_o, recalling

that $M_o=\int_0^\infty dx\int_0^\infty d\alpha\ \mathbf{q}^*(x,\alpha)\mathbf{F}(x,\alpha)$. Also, $a_{\rm nuc}(x)$ can differ significantly from $\mu a(x)=\mu\int_0^\infty d\alpha\ \alpha\mathbf{F}(x,\alpha)/f(x)$ due to the weighting by $\mathbf{q}^*$.

For the 'nucleation-within-a-cell' picture, with $M_o=1$ and $A_{\rm nuc}(s,A)=\lambda A$, the above shows that $a_{\rm avnuc}\neq\lambda$. Nonetheless, λ and $a_{\rm avnuc}$ may still be comparable. Suppose that $a_{\rm nuc}(x)=\lambda a(x)$ [where still $a_{\rm avnuc}\neq\lambda$, since $\int_0^\infty f(x)a(x)q^*(x)dx\neq 1$], and make the approximate identification that $a_{\rm avnuc}=a(0)$ (cf. Sec. III). Then one has $\lambda^{-1}=\int_0^\infty dx\ f(x)q^*(x)[a(x)/a(0)]>1$, since $a(x)/a(0)>1$ and $\int_0^\infty dx\ f(x)q^*(x)=1$. Using fitted scaling functions for point-island simulation data, this relation provides an estimate of $\lambda\approx 0.7$, which is close to $a_{\rm avnuc}\approx 0.9$. We also note that setting λ constant [e.g., $\lambda\approx 0.4$ from MR (Ref. 12)] is not likely to be accurate (cf. Fig. 7).

Finally, we comment on the issue of θ-independent scaling. A reasonable lowest-order approximation is that both $Q^*_{s,A}$ and $A_{\rm nuc}(s,A)$ should depend primarily on the free area, $A^f=A-s$ of the cell within which nucleation occurs (noting that $A_{\rm nuc}<A^f$). Then the associated scaling functions would depend primarily on $A^f/A_{\rm av}=\alpha-\theta x$, and thus carry an explicit θ dependence. This would preclude precise θ-independent scaling of $\mathbf{F}$ (except for $\theta\ll 1$). However, in practice, there is a strong correlation between s and A, so a dependence on $A^f/A_{\rm av}$ may be reasonably approximated by a dependence on $A/A_{\rm av}=\alpha$.

APPENDIX D: SCALING OF THE TOTAL CELL AREA DISTRIBUTION

Here we assume a θ-independent scaling (cf. Ref. 10), and consider the behavior of the total cell area distribution, $N_A=\Sigma_{s>1}N_{s,A}$. This distribution is characterized by the scaling function $g(\alpha)=\int_0^\infty dx\ \mathbf{F}(x,\alpha)$ which satisfies $\int_0^\infty d\alpha\ g(\alpha)=1$. For reference, simulation results for $g(\alpha)$, for point islands using VC's, and square islands using EC's, are shown in Fig. 11. For simplicity, we adopt the nucleation-in-a-cell picture of Sec. IV F. Applying $\int_0^\infty dx\cdot$ to Eq. (32) yields

$$\begin{aligned}2g(\alpha)+\alpha\partial/\partial\alpha\ \ g(\alpha)&=(1-\varpi)^{-1}\mathbf{C}_{\rm tot}(0,\alpha)\mathbf{F}(0,\alpha)\\&\quad+\int_0^\infty dx[\mathbf{q}^*(x,\alpha_+)\mathbf{F}(x,\alpha_+)d\alpha_+/d\alpha\\&\quad-\mathbf{q}^*(x,\alpha)\mathbf{F}(x,\alpha)]\\&=\int_0^\infty dx[\mathbf{q}^*(x,\alpha'_+)\mathbf{F}(x,\alpha'_+)d\alpha'_+/d\alpha\\&\quad+\mathbf{q}^*(x,\alpha_+)\mathbf{F}(x,\alpha_+)d\alpha_+/d\alpha-\mathbf{q}^*(x,\alpha)\mathbf{F}(x,\alpha)].\end{aligned}\tag{D1}$$

In the last line, we applied boundary condition (43) to eliminate $\mathbf{C}_{\rm tot}(0,\alpha)\mathbf{F}(0,\alpha)$, and also to achieve *cancellation* of the factor $(1-\varpi)$, so the quantity ϖ does *not* appear explicitly in Eq. (D1).

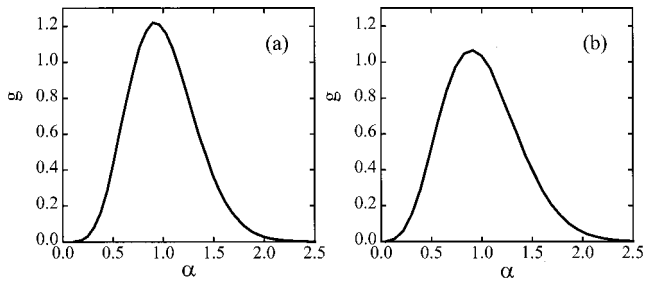

FIG. 11. Simulation results for $g(\alpha)$ for (a) point islands using VC's, and (b) square islands using EC's, at 0.1 ML with $h/F=10^7$.

To proceed further, we make the simplifying MR-type assumptions that $\alpha_{\rm nuc}(x,\alpha)=\lambda\alpha$ and $\mathbf{q}^*(x,\alpha)=c\alpha^4$. Below, for convenience, we set $\lambda'=1-\lambda$. Then Eq. (D1) reduces to

$$\begin{aligned}\alpha\partial/\partial\alpha g(\alpha)&=(c/\lambda)(\alpha/\lambda)^4 g(\alpha/\lambda)+(c/\lambda')\\&\quad\times(\alpha/\lambda')^4 g(\alpha/\lambda')-c\alpha^4 g(\alpha)-2g(\alpha).\end{aligned}\tag{D2}$$

Then, applying the integration $\int_0^\infty d\alpha\cdot$ to Eq. (D2) yields $c\int_0^\infty d\alpha\ \alpha^4 g(\alpha)=1$, which is the normalization condition used to determine c (cf. Appendix C). Dividing Eq. (D2) by α and then integrating $\int_0^\infty d\alpha\cdot$ using the natural boundary conditions that $g(0)=g(\infty)=0$, implies the constraint that

$$c(1/\lambda+1/\lambda'-1)\int_0^\infty d\alpha\ \alpha^3 g(\alpha)=2\int_0^\infty d\alpha\ g(\alpha)/\alpha.\tag{D3}$$

One might attempt to use Eq. (D2) iteratively to generate a solution, so the ith iterate g_i is fed into the RHS, and the $(i+1)$st iterate g_{i+1} appears on the LHS. However, iteration does not necessarily preserve Eq. (D3). A nontrivial solution to Eq. (D3) exists if the PDE [Eq. (32)] with boundary condition (43) has a solution. However, this is not proven (and is not obvious since the PDE equation involves approximations). It is plausible that solutions exist only for certain λ.

APPENDIX E: CLOSURE AND SOLUTION OF MOMENT EQUATIONS

A complete analysis of the moment equations in Sec. IV D for $f(x)$, $a(x)$, and $\sigma^2(x)$ requires some closure approximation for higher moments $\int_0^\infty\alpha^n\mathbf{F}\ d\alpha$, with $n>2$. One strategy is to set to zero the third- and higher-order *cumulants* of $\mathbf{F}$ vs α, for each fixed x (i.e., to assume Gaussian cell area distributions). To simplify this analysis, we adopt the MR from for $\mathbf{q}^*(x,\alpha)=c\alpha^4$, where $c\approx 0.64$ (see Appendix C), and write $\alpha_{\rm nuc}(x,\alpha)=\lambda(x)\alpha$ (generalizing the theory of MR). Then the integrands in the nucleation terms in Eqs. (37) and (40) reduce to the simple high-order moments

$$\int_0^\infty d\alpha\ \alpha_{\rm nuc}\mathbf{q}^*\mathbf{F}=\lambda c\int_0^\infty d\alpha\ \alpha^5\mathbf{F}\approx\lambda c(a^5+10a^3\sigma^2+15a\sigma^4)f\equiv m(x)f(x), \tag{E1}$$

and

$$\int_0^\infty d\alpha\ \alpha_{\rm nuc}(2\alpha-\alpha_{\rm nuc})\mathbf{q}^*\mathbf{F}=\lambda(2-\lambda)c\int_0^\infty d\alpha\ \alpha^6\mathbf{F}\approx\lambda(2-\lambda)c(a^6+15a^4\sigma^2+45a^2\sigma^4+15\sigma^6)f\equiv n(x)f(x). \tag{E2}$$

Note that $m(x)\equiv a_{\rm nuc}(x)q^*(x)$. After substituting Eq. (E1) into Eq. (37), and Eq. (E2) into Eq. (40), it is straightforward to use Eq. (35) to eliminate $f(x)$, yielding a coupled closed pair of first-order ODE's:

$$[(a-\varpi x)-\sigma^2(a-\varpi x)^{-1}]da/dx+d/dx(\sigma^2)=(1-\varpi)(a-m)-\sigma^2(2\varpi-1)(a-\varpi x)^{-1}, \tag{E3}$$

$$[2a(a-\varpi x)-2\varpi x\sigma^2(a-\varpi x)^{-1}]da/dx+(3a-\varpi x)d/dx(\sigma^2)=-(1-\varpi)n-\sigma^2[6(\varpi-2/3)a+2(1-\varpi)\varpi x]\times(a-\varpi x)^{-1}+2(1-\varpi)a^2. \tag{E4}$$

Integrating Eqs. (E3) and (E4) produces reasonable behavior for small x, but the solution becomes singular with $a-\varpi x\to 0$, at finite x. This reflects in part the inadequacy of our description in Eqs. (E1) and (E2) of the nucleation terms.

[1] J. A. Venables, Philos. Mag. **27**, 693 (1973).

[2] S. Stoyanov and D. Kashchiev, Curr. Top. Mater. Sci. **7**, 69 (1981).

[3] G. S. Bales and D. C. Chrzan, Phys. Rev. B **50**, 6057 (1994).

[4] M. C. Bartelt and J. W. Evans, Phys. Rev. B **46**, 12 675 (1992); Surf. Sci. **298**, 421 (1993); and in *Common Themes and Mechanisms of Epitaxial Growth*, edited by P. Fuoss, J. Tsao, D. W. Kisker, A. Zangwill, and T. Kuech, MRS Symposia Proceedings, No 312 (Materials Research Society, Pittsburgh, 1993), p. 255; J. W. Evans and M. C. Bartelt, J. Vac. Sci. Technol. A **12**, 1800 (1994).

[5] J. G. Amar and F. Family, Phys. Rev. Lett. **74**, 2066 (1995) proposed that $f(x)\propto x\exp[-2.7x^{3.7}]$ for irreversible island formation, so that $f(0)=0$, in contrast to our theory.

[6] P. A. Mulheran and J. A. Blackman, Philos. Mag. Lett. **72**, 55 (1995); Phys. Rev. B **53**, 10 261 (1996).

[7] M. C. Bartelt and J. W. Evans, Phys. Rev. B **54**, R17 359 (1996); and in *Structure and Evolution of Surfaces*, edited by R. C. Cammarata, E. H. Chason, T. L. Einstein, and E. D. Williams, MRS Symposia Proceedings No. 440 (Materials Research Society, Pittsburgh, 1997), p. 247.

[8] M. C. Bartelt, A. K. Schmid, J. W. Evans, and R. Q. Hwang, Phys. Rev. Lett. **81**, 1901 (1998); and in *Mechanisms and Principles of Epitaxial Growth in Metal Systems*, edited by L. C. Wille, C. P. Burmester, K. Terakura, G. Comsa, and E. D. Williams, MRS Symposia Proceedings No. 528 (Materials Research Society, Pittsburgh, 1998), p. 253.

[9] M. C. Bartelt, C. R. Stoldt, C. J. Jenks, P. A. Thiel, and J. W. Evans, Phys. Rev. B **59**, 3125 (1999).

[10] D. D. Vvedensky, R. E. Caflisch, M. F. Gyure, B. Merriman, S. Osher, C. Ratsch, and J. J. Zinck, in *Mechanisms and Principles of Epitaxial Growth in Metal Systems* (Ref. 8), p. 261; R. E. Caflisch, M. F. Gyure, B. Merriman, S. J. Osher, C. Ratsch, D. D. Vvedensky, and J. J. Zinck, Appl. Math. Lett. **12**, 13 (1999); D. D. Vvedensky, Phys. Rev. B **62**, 15 435 (2000).

[11] J. W. Evans and M. C. Bartelt, in *Morphological Organization in Epitaxial Growth and Removal*, edited by Z. Zhang and M. G. Lagally (World Scientific, Singapore, 1998).

[12] P. A. Mulheran and D. A. Robbie, Europhys. Lett. **49**, 617 (2000).

[13] C. Ratsch, M. F. Gyure, S. Chen, M. Kang, and D. D. Vvedensky, Phys. Rev. B **61**, R10 598 (2000).

[14] M. C. Bartelt, J. B. Hannon, A. K. Schmid, C. R. Stoldt, and J. W. Evans, Colloids Surf., A **165**, 373 (2000).

[15] See Ref. 18 of Phys. Rev. B **54**, R17 359 (1996) (Ref. 7).

[16] In general, one has $[1+(n-1)\varpi]\int_0^\infty dx\,x^n f(x)=n\int_0^\infty dx\,x^{n-1}C_{\rm tot}(x)f(x)$, for $n\geq 1$, assuming the integrability of $x^n f$ and $x^{n-1}C_{\rm tot}f$.

[17] G. S. Bales (unpublished).

[18] This complication applies for capture zones of compact islands chosen as EC's and DC's, but not for VC's. See Sec III C. It does not apply for point islands.

[19] See *Morphological Organization in Epitaxial Growth and Removal* (Ref. 11) for a derivation, but note the error in the coefficients of the $a(x)$ equation.

[20] Assuming that point-island-like behavior must be achieved for EC-tessellations of compact island distributions at very low θ (where VC's and EC's coincide), it follows that $C_{\rm tot}(x)\approx\gamma a(x)+(1-\gamma)$, with $\gamma\approx 0.7$, for $\theta\ll 1$ (see Ref. 7), increasing to $\gamma\approx 1$, for higher θ.

[21] G. M. Murphy, *Ordinary Differential Equations and their Solutions* (Van Nostrand, Princeton, 1960), pp. 23–26.

[22] J. W. Evans, J. B. Hannon, M. C. Bartelt, and G. L. Kellogg, Bull. Am. Phys. Soc. **45**, 363 (2000).

[23] One must use that the inverse function for α'_+ is $\alpha_{\rm nuc}$. See Appendix C.

[24] F. G. Gibou, C. Ratsch, M. F. Gyure, S. Chen, and R. E. Caflish, Phys. Rev. B **63**, 115401 (2001).

[25] For $n>2$, one has $(2s-4)c_s=c_{s-1}-3[5\times 7\times 9\times\ldots\times(2s-1)]^n\lambda(c_s)^{n+1}$.

[26] Note that $A_s/A_{\rm av}=[(2s-1)/(2s-4+3\lambda)](A_{s-1}/A_{\rm av})$, for $n=0$.